THEMIS observations of consecutive bursts of Pi2 pulsations: The 20 April 2007 event

C.-C. Cheng,[1] C. T. Russell,[2] V. Angelopoulos,[2] I. Mann,[3] K. H. Glassmeier,[4] U. Auster,[4] and W. Baumjohann[5]

[1]   On 20 April 2007, four Pi2 pulsation bursts occurred successively and simultaneously in the premidnight sector at the E spacecraft and ground-based observatories for the THEMIS mission, while the *AE* index was less than 100 nT. Especially for the last three onsets, both ground-based and GOES 12 magnetometers sensed magnetic perturbations, as expected from the formation of a substorm current wedge (SCW). Moreover, LANL 1994−084 detected an enhancement of energetic particle flux. Spectral analysis shows a matched wave frequency ∼6−8 mHz and another harmonic frequency ∼17 mHz for the fourth burst. The orientation of the major axis of the wave polarization hodogram points toward the SCW location. The first burst has both latitudinal and longitudinal polarization changes from counterclockwise (CCW) to clockwise (CW), in contrast to the other three that have a latitudinal reversal only. The longitudinal CW to CCW change at low latitudes signifies that hydromagnetic waves propagate westward and eastward from the longitude of the impulsive source responsible for SCW. The latitudinal CW to CCW reversal is consistent with induction by a westward moving upward field-aligned current carried by Alfvén waves leading to field line oscillations. Consequently, they can be explained by the coupling of a fast magnetospheric cavity mode driven by fast compressional waves to field line resonances as expected from braking bursty bulk flows, resulting from magnetotail reconnection, triggered by a preceding northward interplanetary magnetic field turning. This event shows that the source mechanism of consecutive Pi2 onsets at times of weak geomagnetic activity is the same as during substorm times.

1.   Introduction

[2]   Recurrent onsets in an associated disturbance sequence are a common phenomenon, but their cause remains poorly understood. Before the advent of spaceborne measurements, ground magnetometers recorded multiple bursts of Pi2 pulsations with periods 40−150 s occurring in succession during substorms (see the review by *Saito* [1969]). Subsequently, *Clauer and McPherron* [1974] reported evidence of multiple onsets accompanied by Pi2 pulsations in a magnetospheric substorm.

[3]   Recent studies [*Sutcliffe*, 1998; *Sutcliffe and Lyons*, 2002] showed that a train of Pi2 pulsations can occur at high and low latitudes during quiet times. In particular, *Sutcliffe and Lyons* [2002] pointed out their association with poleward boundary intensifications (PBIs) and enhancements of energetic particle fluxes in the plasma sheet. However, there are a couple of observational results not explained by *Sutcliffe and Lyons* [2002] (hereinafter referred to as SL02). One unexplained result may be seen in Figure 1 of SL02, in which the first Pi2 burst can be clearly found at the low latitude station but not at the high-latitude one. The other unexplained result may be seen in Figure 4 of SL02, in which the amplitude of low-latitude Pi2s seems inconsistent with the intensity of associated magnetic disturbances at high latitudes, PBIs, and the flow bursts in the plasma sheet. In addition, *Rostoker* [2000] demonstrated that both Pi2s and weak substorm activity could occur along the nightside auroral oval during an interval of low solar wind pressure. Since the magnetic disturbance at the equatorward edge of the oval was not the same as the disturbance at the poleward edge, consistent with their being PBIs, *Rostoker*

---

[1]Faculty of Physics, National Formosa University, Hu-Wei, Taiwan.
[2]Institute of Geophysics and Planetary Physics, University of California, Los Angeles, California, USA.
[3]Department of Physics, University of Alberta, Edmonton, Alberta, Canada.
[4]Institute for Geophysics and Extraterrestrial Physics, Technical University of Braunschweig, Braunschweig, Germany.
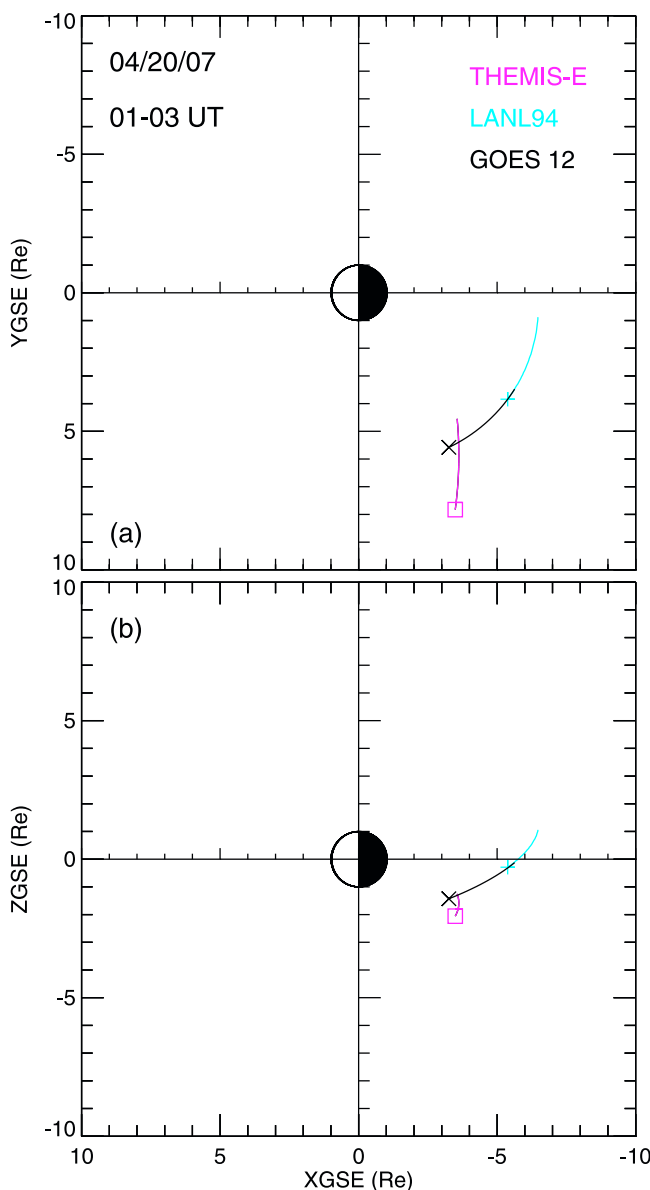[5]Space Research Institute, Austrian Academy of Sciences, Graz, Austria.

Figure 1. The locations of THEMIS-E, LANL 94, and GOES 12 in GSE (a) X–Y and (b) X–Z coordinates from 0100 UT to 0300 UT on 20 April 2007.

[2000] suggested that they could be independent and might have different physical origins.

[4] When the solar wind interaction with the Earth's magnetosphere is weak, one may expect that the input of external momentum is not strong enough to cause substorm or substorm-like activations. One would even take a view that the cause of quiet time Pi2s is different from those triggered by the interplanetary magnetic field (IMF) variation during substorm times. Thus, it is an important issue in magnetospheric physics to distinguish whether quiet time Pi2s (or substorm-like activations) are internally or externally excited.

[5] According to *Sutcliffe and Lyons* [2002], the quiet time event has a repetitive period of ~30 min, similar to those events that occurred during prolonged periods of

strongly southward and relatively steady IMF. *Rostoker* [2000] contended that the quiet time ULF activity might be driven by IMF fluctuations with the coupling of cavity resonances to field lines in the higher latitude region of the plasma sheet. But these previous studies did not investigate further IMF variation effect on quiet time events. Thus, the cause of quiet time Pi2s may be associated with IMF variations, like those during substorm onsets, as studied by *Cheng et al.* [2002a, 2002b, 2005]. Recently, *Cheng et al.* [2009] investigated the relationships of quiet time Pi2s with IMF variations by using three previously published events. They argued that quiet time Pi2s in the nightside magnetosphere can be the same as ones caused by the impulsive source in the magnetotail associated with the IMF variation, and not be excited internally during substorm times. However, their arguments are qualitative and not quantitatively justified for lack of high resolution data at geostationary orbit and in the near-Earth magnetotail.

[6] On 20 April 2007, the THEMIS-E spacecraft moved inbound at the dusk flank of the nightside magnetosphere, GOES 12 and LANL 1994–084 (denoted as LANL 94 hereinafter) at the geostationary altitude orbiting in the premidnight sector. These multipoint observations at geostationary orbit and in the dusk sector of the nightside magnetosphere were coincidentally well coordinated to compare with ground magnetic measurements. THEMIS-E is one of the five-probe constellations, equipped with the magnetic sensors with an unprecedented sensitivity better than 0.1 nT, for the mission of Time History of Events and Macroscale Interactions during Substorms [see *Angelopoulos*, 2008]. This provides us an opportunity to make a quantitative examination of the suggestion by *Cheng et al.* [2009].

2. Data Presentation

2.1. THEMIS-E and Geostationary Observations

[7] Figures 1a and 1b show the locations of THEMIS-E, GOES 12 and LANL 94 in GSE X–Y and X–Z coordinates during the period from 0100 UT to 0300 UT on 20 April 2007, respectively. During the time of interest, THEMIS-E spacecraft moved earthward at the dusk side magnetosphere while at geostationary altitude, GOES 12 and LANL 94 respectively crossed local time sectors of 2000–2200 and 2130–2330. Figure 2 shows that the foot points (red marks) of THEMIS-E during the time of interest were around the GILL ($L = 6.13$, corrected geomagnetic latitude 67.39° and corrected geomagnetic longitude 339.49°) station using the *Tsyganenko* [1989] model. One can see from Figure 2 that the foot points of THEMIS-E get closer to GILL as it moves more earthward.

[8] Figures 3a–3c show three components of the magnetic perturbations in GSE coordinates, filtered in the Pi2 period band, detected by THEMIS-E during the time from 0100 UT to 0300 UT on 20 April 2007. Details of instrumentation and measurements of the fluxgate magnetometer on board THEMIS-E are given by *Auster et al.* [2008]. One can determine that there were four Pi2 bursts occurring at 0122 UT, 0211 UT, 0234 UT and 0243 UT, respectively. At THEMIS-E, the last three bursts had clear wave perturbations in all three components of the magnetic field, in contrast to the first one which had perturbations in the B_x and B_z components only. In this study, the vertical
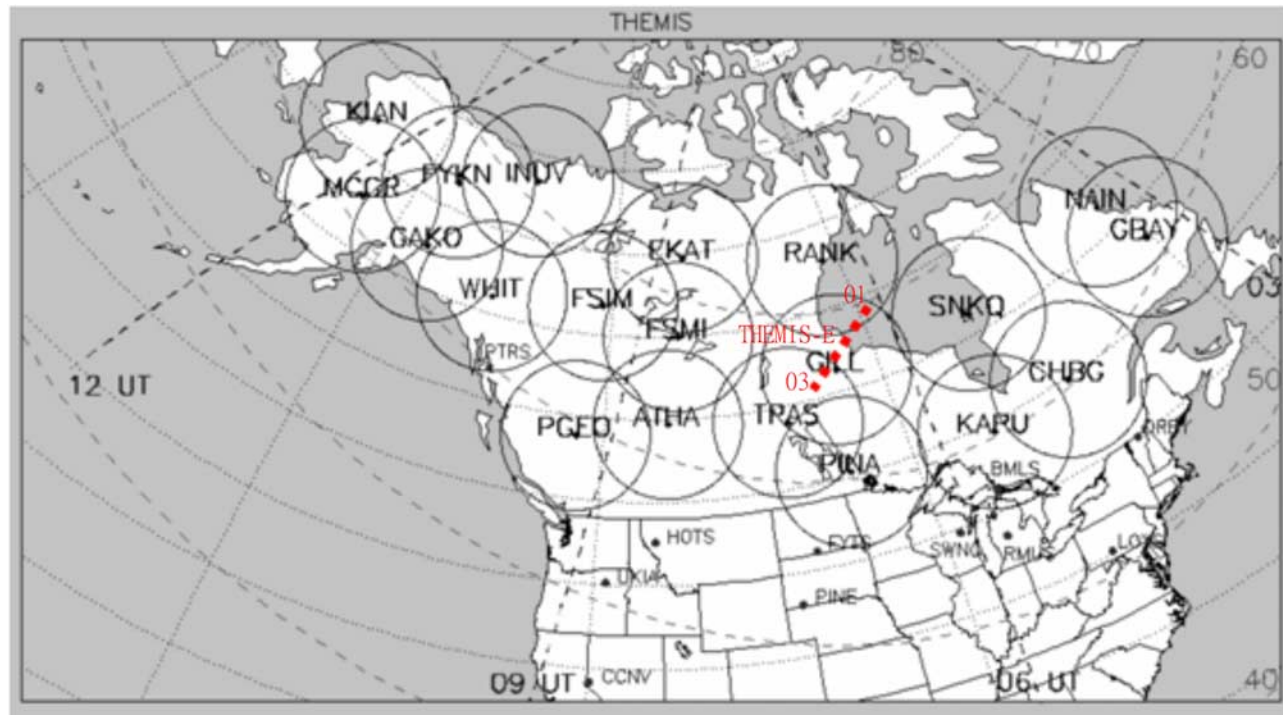
Figure 2. The locations of the ground-based observatories for the THEMIS mission and the THEMIS-E foot points (red marks) from 0100 UT to 0300 UT on 20 April 2007.

dashed line denotes the onset of the Pi2 bursts that are marked with numbers for reference. Figure 3d shows the *AE* index derived from the ground magnetometer data of the THEMIS mission. A detailed description of THEMIS ground-based magnetometers is provided by *Russell et al.* [2008]. Notably, each Pi2 burst appeared at a time when the *AE* index was less than 100 nT.

[9] Figures 3e–3h display the time derivative of the *H* component, filtered in the Pi2 period band, observed at the ground stations close to the foot points of THEMIS-E during the time of interest. From Figure 3, one can clearly determine that four consecutive Pi2s occurred simultaneously at THEMIS-E and the ground stations. Figure 4 shows the time series of the *H* and *D* components from the high to low latitude stations at the longitude closest to the THEMIS-E foot points. In contrast to the occurrence at other stations, strong magnetic bays in the *H* component strongly occurred at GILL ($L = 6.13$) at each Pi2 onset. At lower latitudes, burst 1 occurred with a clear but weak wave fluctuation in the *D* component, in contrast to that at RANK ($L = 10.95$) (see Figure 15 for a closer look). As for bursts 2, 3, and 4, the fluctuation amplitude in the *D* component became larger than that in the *H* component for the low *L* stations. Moreover, the *D* component became more enhanced at lower latitudes at burst 2 onset than the *H* component. For bursts 3 and 4, the *D* component first became enhanced at ~0234 UT. This enhancement was accompanied by a small amplitude wave perturbation that later intensified with a larger amplitude after burst 3 onset when the magnetic bay in the *H* component began. The enhancements in the *D* component are consistent with those reported by *Sakurai and McPherron* [1983]. Except for burst 1, these ground observations signify the occurrence of the westward electrojet and the upward field-aligned current, like those during substorms. The comparison of THEMIS-E and ground observations also shows that the onset of ground Pi2s has a one-to-one relationship with those in space. Hence, the generation and propagation mechanisms of these Pi2 bursts can be closely related to one another, and they resemble those during substorm times.

[10] Figures 5a–5c show three components of the magnetic field sensed by GOES 12. The magnetic field at GOES 12 is defined as *Hp*, perpendicular to the satellite orbital plane (or parallel to the Earth spin axis in the case of a zero degree inclination orbit); *He*, perpendicular to *Hp* and directed earthward; and *Hn*, perpendicular to *Hp* and directed eastward. One can see from Figure 5a that the *He* component had a wave-like fluctuation after each Pi2 onset from 0100 UT to 0300 UT (corresponding to 2000 LT to 2200 LT). But in Figures 5b and 5c, the *Hn* and *Hp* components became perturbed only after the last three onsets. Notably, the *Hp* component was enhanced with a delay time ~4 min to burst 2 onset. Moreover, like the THEMIS-E and ground observations, the magnetic perturbations at GOES 12 began at burst 3 onset and persisted through the duration time of burst 4. These observations imply the formation of a current wedge, like those during substorms.

[11] We also scanned the energetic particle measurements at geostationary orbit to see if there were any injections in association with the formation of the substorm-like current wedge. During the time of interest, the LANL-94 satellite passed through the local time sector of 2130–2330. Figures 5d and 5e show the electron flux in two energy ranges of 50–225 keV and 315–1500 keV detected by LANL 94. One can find from Figures 5d and 5e that the electron flux does not have a clear enhancement at burst 1 onset, but tends to
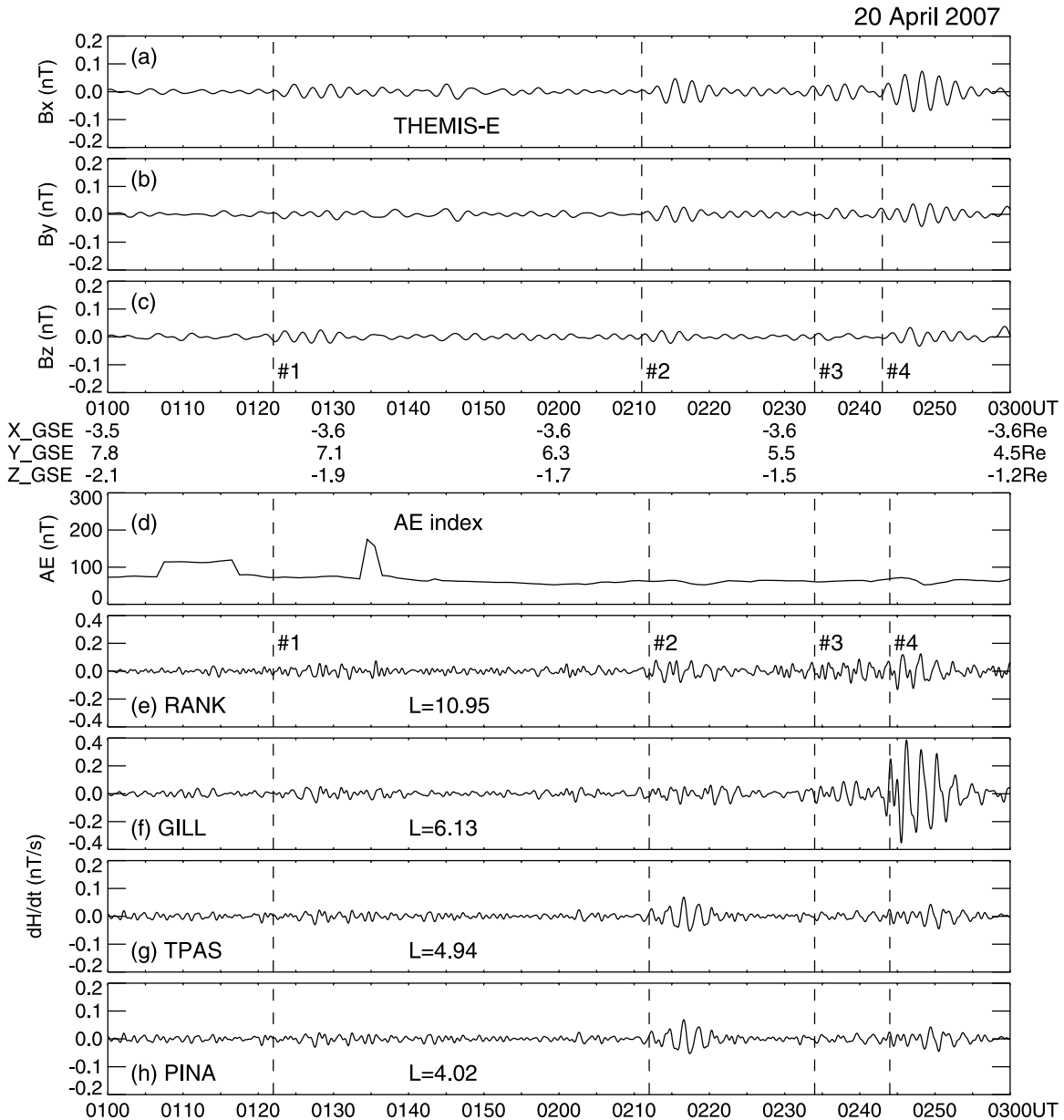
Figure 3. THEMIS observations from 0100 UT to 0300 UT on 20 April 2007. (a–c) The time derivative of three components of the magnetic field in GSE coordinates sensed by THEMIS-E. (d) The THEMIS *AE* index. (e–h) The time derivative of the *H* component at the ground-based observatories close to the THEMIS-E foot points. The vertical dashed lines denote the Pi2 onsets. Four consecutive Pi2 bursts are marked with a serial number, respectively.

become enhanced after the onsets of bursts 2–4. By comparing Figure 5c to Figure 5d, one can find that the enhanced *Hp* component followed the enhancement of the electron flux in 50–225 keV. But a comparison of Figures 5a and 5e shows that the perturbed *He* component occurred simultaneously with the enhancement of the electron flux in 315–1500 keV. A similar phenomenon recurred at ∼0235 UT for the *Hp* component in Figure 5c, compared with electron flux in 50–225 keV in Figure 5d. The latter, especially, became stronger after burst 4 onset. These observational results show that enhanced disturbances at geostationary orbit are closely related to the formation of substorm-like current wedges at the last three Pi2 onsets and

hence imply that their source mechanisms can be like those at substorm times.

2.2. Spectral Analysis

[12] To further verify that their source mechanisms are the same as those during substorm times, we analyze the power spectrum of four Pi2 bursts detected at THEMIS-E and the GILL (*L* = 6.13) station in this section. The time span for analysis is 10 min by starting at 0120 UT for burst 1, 0210 UT for burst 2, 0230 UT for burst 3, and 0240 UT for burst 4. Figures 6a–6d show the spectral amplitude of the three components measured at THEMIS-E in the dipole meridian system with a coordinate transformation by *Kivelson and*
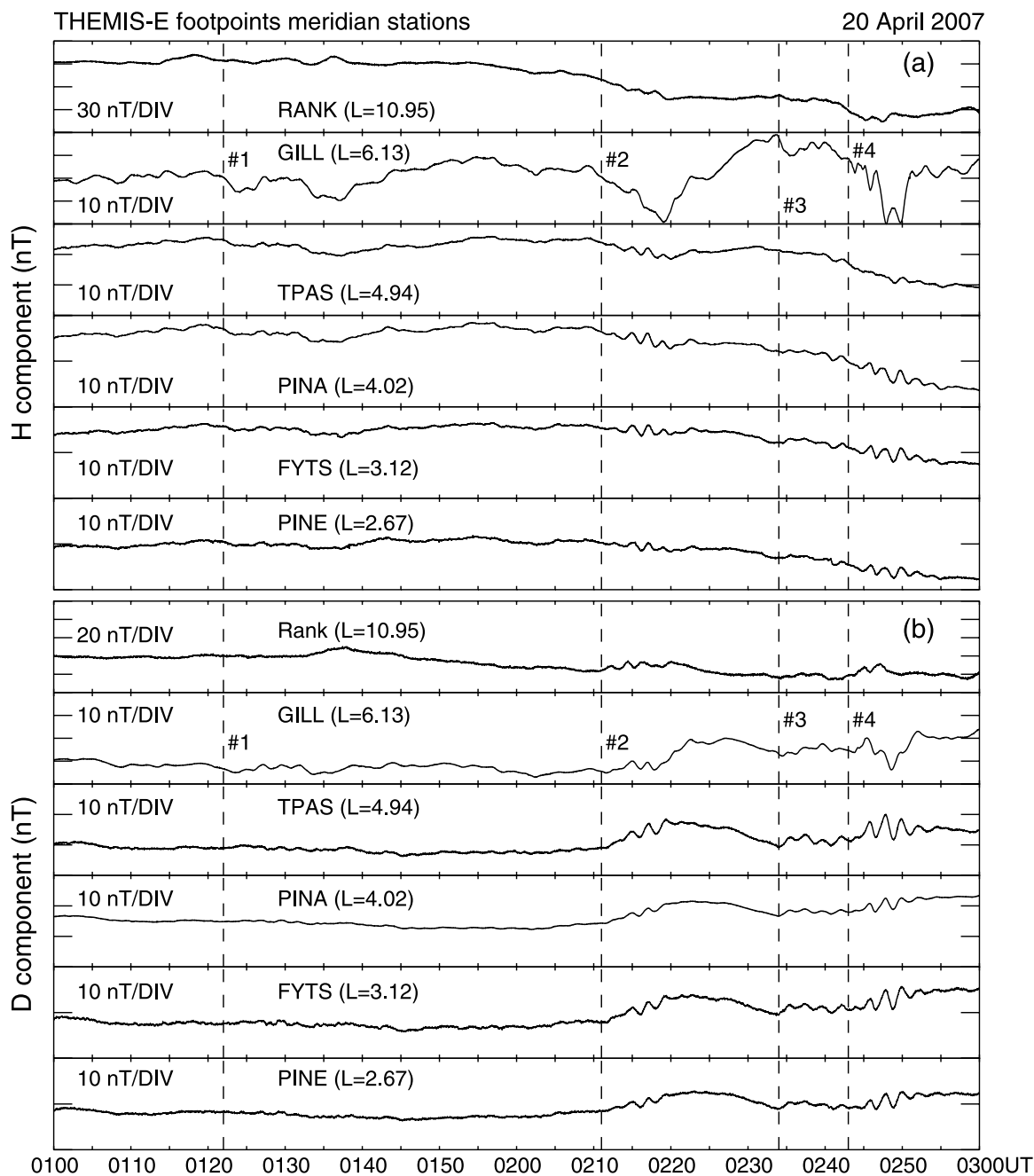
Figure 4. The (a) *H* and (b) *D* components at the ground-based observatories along the longitude close to the THEMIS-E foot points. The vertical dashed lines denote the Pi2 onsets. Four consecutive Pi2 bursts are marked with a serial number, respectively.

Russell [1995]. In Figures 6a–6d, the dash-dotted trace is the *Br* component directed outward from the Earth's dipole axis, the dotted trace is the *Bn* component in the eastward direction, and the dashed trace is the *Bp* component along the geomagnetic north. Figures 6e–6h show the spectral amplitude of *H* and *D* components recorded by the GILL magnetometer. In Figures 6e–6h, the dotted trace denotes the *D* component, and the dashed trace represents the *H* component. For burst 1, the amplitude of three components at THEMIS-E is largest at a frequency of ~6.5 mHz (marked with a vertical line) that matches the second peak frequency of the *H* component at GILL. Moreover, the *H*

and *D* components at GILL have two harmonic peaks in contrast to THEMIS-E. As for burst 2, the *Br* component at THEMIS-E has a peak frequency ~8 mHz (marked with a vertical line) and the *Bn and Bp* components at ~9 mHz instead. At GILL, the *H* and *D* components have a peak frequency of ~6 mHz and ~8 mHz (marked with a vertical line). One can find from Figure 6c that the spectral amplitude of burst 3 is weak and enhanced at the frequency ~6.5 mHz for the *Br* component and ~13 mHz for *Bp* (marked with two vertical lines). Different from the *D* component with one largest peak at ~8 mHz, the *H* component at GILL has three larger peaks at ~2 mHz,
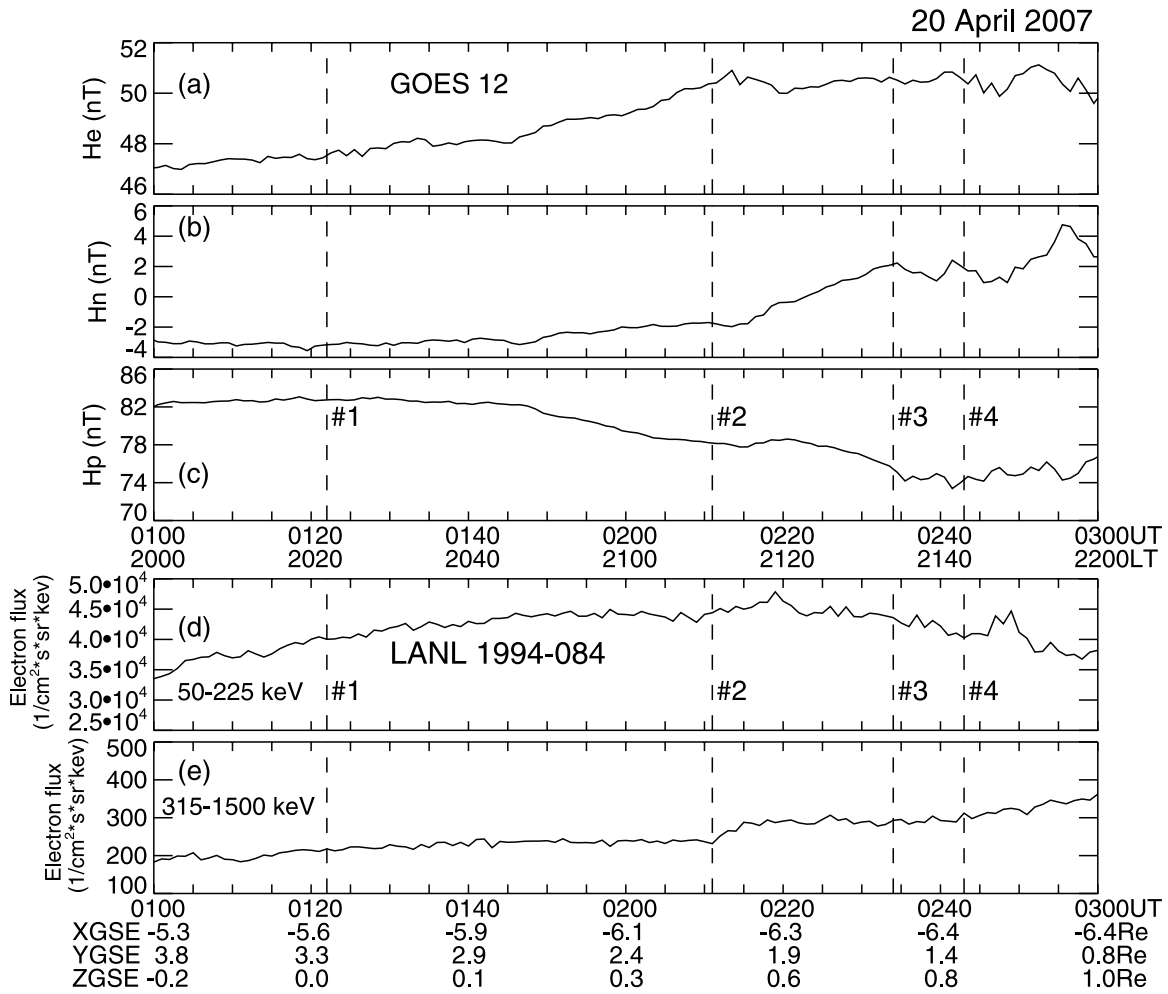
Figure 5. (a–c) The *He, Hn,* and *Hp* components at GOES 12 from 0100 UT to 0300 UT on 20 April 2007. (d) The electron flux in the energy range of 50–225 keV at LANL 1994–084. (e) Same as Figure 5d, except for 315–1500 keV. The vertical dashed lines denote the Pi2 onsets. Four consecutive Pi2 bursts are marked with a serial number, respectively.

∼8 mHz and ∼12 mHz in Figure 6g. Except for the peak at the frequency ∼12 mHz, bursts 1 and 3 at GILL seem to have two similar harmonics. The spectral analysis of burst 4 at THEMIS-E shows two harmonic peaks, one at ∼8 mHz and the other at ∼17 mHz in the *Br* component (marked with two vertical lines), that are the same as that in the *H* component at GILL. Since the spectral analysis of bursts 1, 3, and 4 at GILL shows two harmonic peaks like the ones studied by *Lin et al.* [1991] and *Cheng et al.* [1998, 2000, 2004], this implies that they can result from the fast magnetospheric cavity resonances. However, by comparing Figure 6a to Figure 6e, one finds out that burst 1 at THEMIS-E has the same peak in the three components. At burst 1 onset, there are two magnetic bays in the *H* component at GILL in contrast to other stations in Figure 4. Since no enhancements in the *D* component at low latitudes accompanied the magnetic bay in the *H* component, this indicates that burst 1 may be predominantly affected by the eastward electrojet and not the formation of substorm-like current wedge. *Lester et al.* [1985] suggested that high-latitude Pi2 pulsations can be associated with the eastward electrojet and governed by the field line resonance mecha-

nism while away from the auroral breakup region. Hence, burst 1 seen by THEMIS-E can be excited by the coupling of the fast magnetospheric cavity resonances (corresponding to *Br* and *Bp* components) to field line resonances (corresponding to the *Bn* component).

[13] To justify the above explanation, we also analyzed the power spectrum of four Pi2 bursts observed at the ground stations close to the THEMIS-E foot points. In this study, the first Pi2 burst does not have the perturbations like the ones induced by the substorm-like current wedge. Hence, we proceed to make an extensive analysis only of the last three Pi2 bursts at the ground stations. In the same format as Figure 6, Figures 7, 8, and 9 show the spectral amplitude of *H* and *D* components of the last three bursts at the ground stations from high to low latitudes along the longitude of the THEMIS-E foot points and at the low *L* stations, respectively. In Figures 7, 8, and 9, the dashed trace denotes the *H* component, and the dotted trace represents the *D* component. Moreover, the vertical line denotes the peak frequency detected by THEMIS-E. Except for the *H* component at GILL with the peak frequency ∼6 mHz, there is a clear peak frequency of
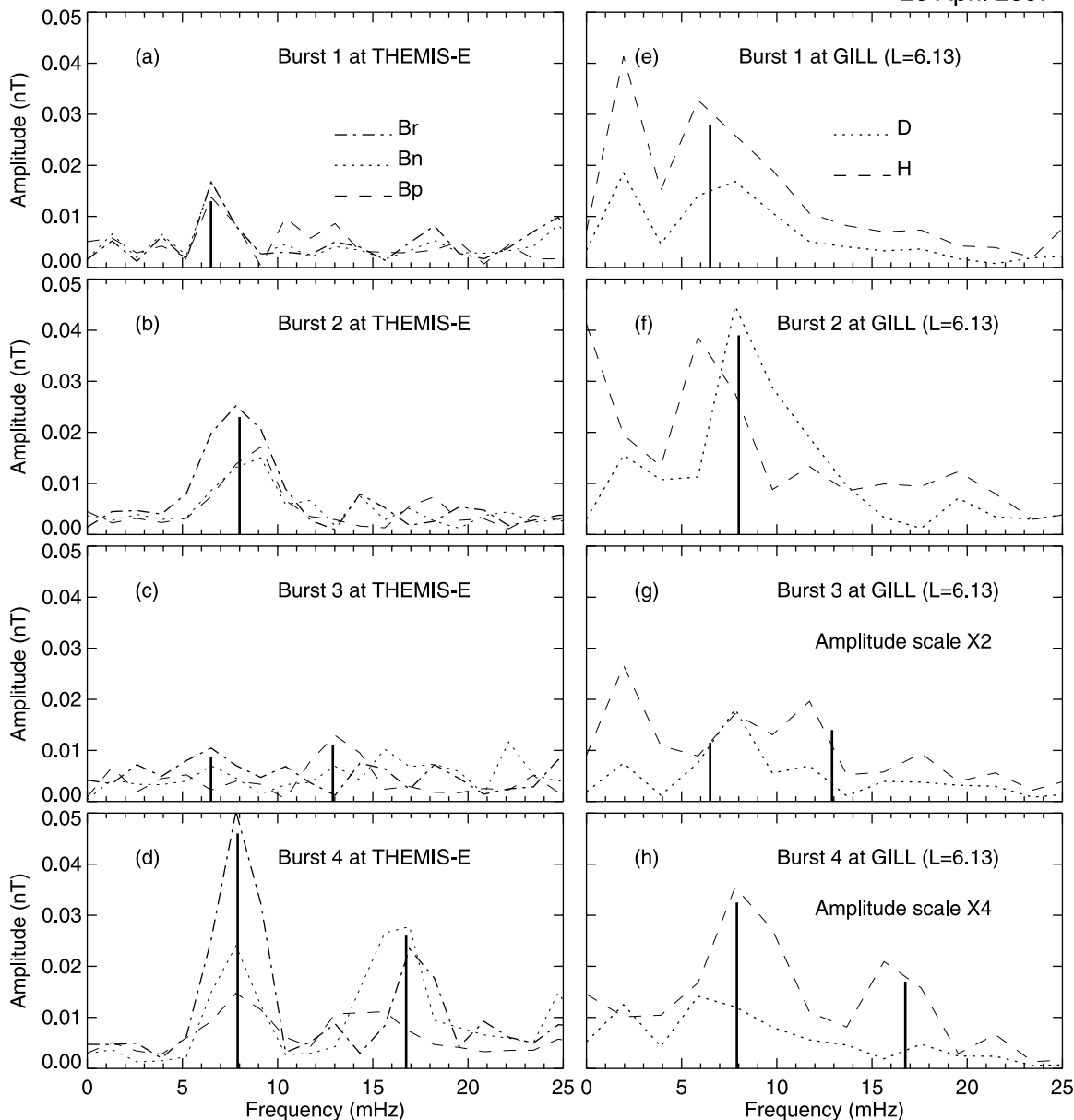
Figure 6. The spectral analysis of four Pi2 bursts at THEMIS-E and GILL ($L = 6.13$). The vertical solid line denotes the peak frequency at THEMIS-E.

$\sim$8 mHz in both components from RANK ($L = 10.95$) to PINE ($L = 2.67$) in Figure 7. The other low-latitude stations at $L \sim 3$ observed the same peak frequency $\sim$8 mHz as that at THEMIS-E for burst 2. Hence, burst 2 may be the fundamental magnetospheric cavity resonance mode. As for GILL, the amplitude of the D component is larger than the H component. According to the ionospheric screening effect proposed by *Hughes and Southwood* [1976], the transverse component in space can be rotated 90° to be the H component on the ground along the ambient magnetic field line. Thus, these waves may be associated with the fundamental magnetospheric cavity resonance mode coupled to the transverse field line resonances.

[14] In the same format as Figure 7, Figure 8 shows the spectral amplitude of H and D components of burst 3. From

Figure 8a, one can see that the spectral amplitude of the H component is larger than the D component at RANK and GILL, in contrast to four other low L stations with the D component more dominant than the H component. Apart from having the first peak at the frequency $\sim$2 mHz, the H component at RANK has the second peak at $\sim$10 mHz larger than $\sim$8 mHz for the D component. As for GILL, there are three peaks in the H component, one of which one is at $\sim$2 mHz same as that at RANK, and the other two being at $\sim$8 mHz same as in the D component and that at RANK and at $\sim$12 mHz not seen by other stations. In Figure 8b, the spectral amplitude of the H component becomes larger than the D component at most low L stations, except for FYTS with the D component larger than the H component. Moreover, the largest spectral peak
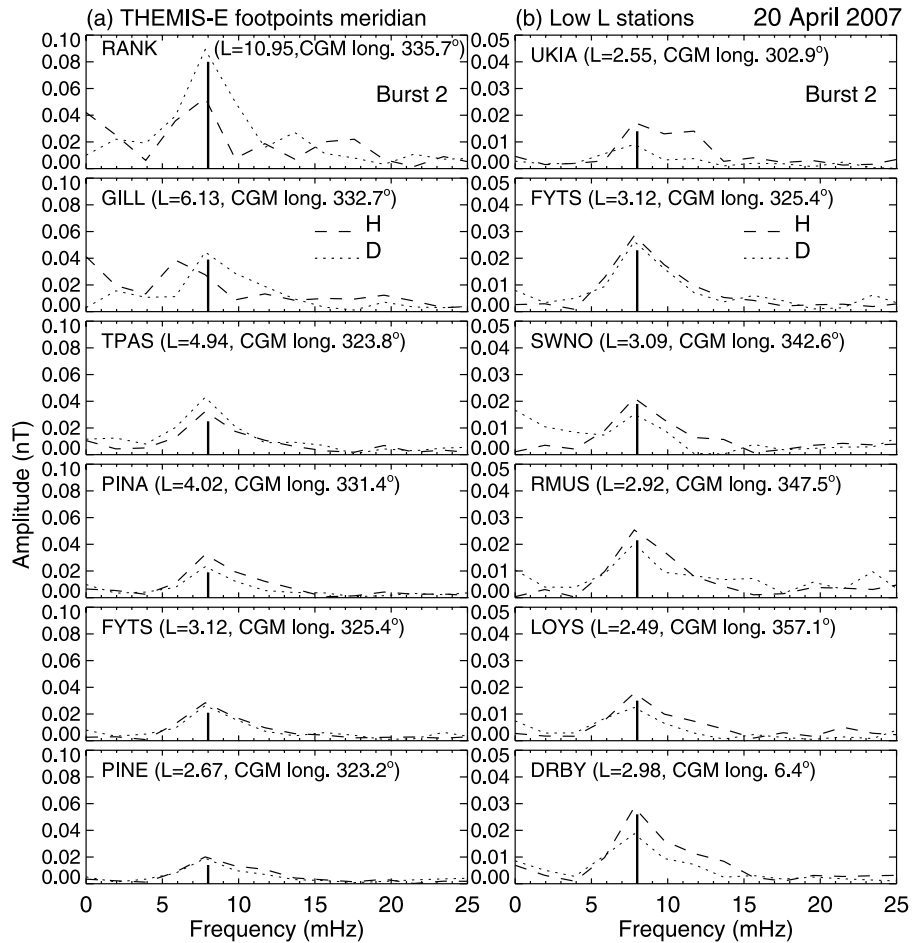
Figure 7. The spectral analysis of the burst 2 at the stations along the longitude close to the THEMIS-E foot points and the low L stations in the spaced longitude. The vertical solid line denotes the peak frequency at THEMIS-E.

is at $\sim$8 mHz for most low L stations, except for UKIA at $\sim$10 mHz. These results indicate that magnetospheric cavity resonances may be responsible for burst 3. In addition, GILL has the other unique spectral peak at $\sim$12 mHz in the H component that could be expected as the surface waves through the coupling to field line resonances, since it is close to the plasmapause.

[15] In the same format as Figure 7, Figure 9 shows the spectral amplitude of H and D components of burst 4. In Figure 9a, there are three peaks in the H and D components at RANK, in contrast to the two at other stations. The amplitude of burst 3 at the stations higher than GILL is larger in the H component than in the D component, but this feature reverses at the TPAS ($L = 4.94$) station. For the stations at lower L than TPAS, the H component is compatible to the D component. In Figure 9b, for the low L stations close to TPAS ($L = 4.94$), the H component is also compatible to the D component. However, for the low L stations away from TPAS, the H component becomes larger than the D component. From Figure 9, one can see that there are two peaks at $\sim$8 mHz and $\sim$17 mHz in the H and D components of burst 4 for all stations. This is the same as the spectral analysis of burst 4 at THEMIS-E.

[16] As a result, ground observations confirm the spectral analysis of four consecutive Pi2 bursts observed at THEMIS-E that the first peak frequency is $\sim$6–8 mHz and the second

peak frequency $\sim$17 mHz. These observational results are the same as those shown by *Lin et al.* [1991] and *Cheng et al.* [1998, 2000, 2004]. Thus, for this event, four consecutive Pi2 bursts can be the coupling of the fast magnetospheric cavity mode driven by fast compressional waves to field line resonances, owing to the impulsive source at the magnetotail like the one during substorms.

2.3. Hodogram Analysis

[17] In addition to the knowledge gained from spectral analysis, the Pi2 hodogram can provide information on the wave propagation and the source location. Figure 10 shows a hodogram of four consecutive Pi2s at THEMIS-E and the ground stations close to the longitude of its foot points. The ground hodogram includes the perturbed H and D components. For THEMIS-E, the hodogram consists of the Br (the compressional component corresponding to the H component) and Bn (the transverse component corresponding to the D component) components projected onto the ground along the ambient magnetic field. One can find out from Figure 10 that the major axis of the wave polarization is oriented to the east, close to the site between RANK and GILL for each Pi2 burst. As for THEMIS-E, bursts 1 and 2 appear linearly polarized. Burst 3 is first linearly polarized and then becomes elliptically polarized as burst 4. The above polarization features at THEMIS-E are consistent
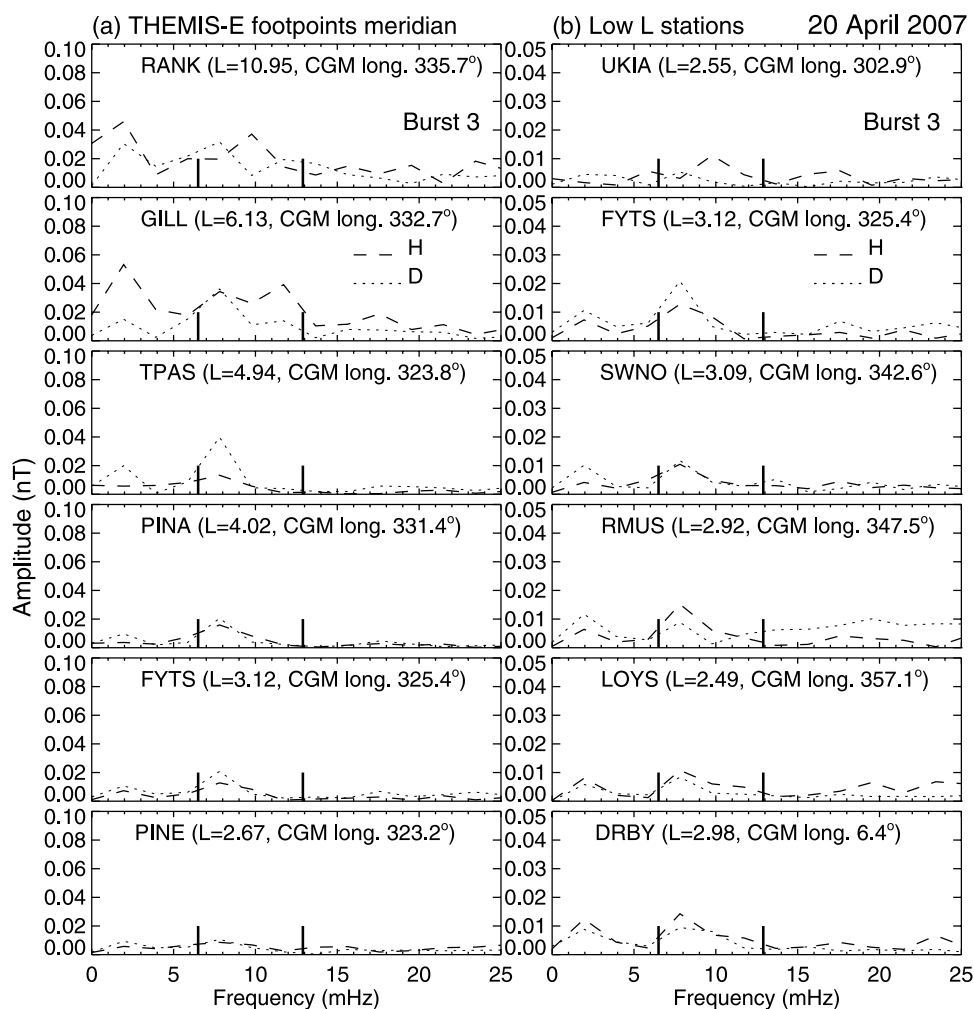
Figure 8. In the same format as Figure 7, except for burst 3.

with the observational results by *Fukunishi* [1975] at the ground stations around the plasmapause foot points. In this study, the hodogram pattern is identified as clockwise (CW) polarization and counterclockwise (CCW) polarization along the direction of the ambient magnetic field. For burst 1, the wave polarization change from CCW at GILL to CW at TPAS. But for bursts 2 and 3, this polarization reversal of CW to CCW occurred between RANK and GILL. A similar polarization change also appeared at burst 4 onset, but down at locations between GILL and TPAS. The polarization pattern of four consecutive bursts at THEMIS-E is orthogonal to the one at the low L stations. Since the polarization reversal occurs at a site close to GILL, the H and D components also have perturbations like the one induced by the westward electrojet and by the upward field-aligned current in the west wing of the substorm-like current wedge. These observational results are consistent with the suggestion by *Pashin et al.* [1982] that the ground polarization can change from CW at the higher latitude than the site of the westward upward field-aligned current to CCW at the lower latitude.

[18] To find out whether the polarization pattern is a global phenomenon like those during substorms, we performed the hodogram analysis at the stations away from the THEMIS-E foot points in both longitude and latitude. In this section, we focus on the hodogram analysis of the second and fourth Pi2 bursts only. Figure 11 shows the wave polarizations at the stations at six spaced longitudes. At the top of each hodogram column is the corrected magnetic longitude of the low L stations longitudinally adjacent to FYTS. One can see from Figure 11 that the wave polarization is CCW at the mid L stations. For the low L stations, the polarization change from CW to CCW occurs between CGM longitude 302.9° and 325.4°. For the low L stations at the longitude beyond CGM longitude 302.9°, the wave polarization remained CCW. In the same format as Figure 11, Figure 12 shows burst 4. Comparing Figure 12 to Figure 11, we find that the polarization patterns are the same. These observational results are also the same as in Figure 1 of *Lester et al.* [1984]. The polarization pattern of Pi2 at mid latitudes is CCW, polarized with the direction of the major axis toward the center of the substorm current wedge. The polarization pattern of the second and fourth Pi2 bursts suggests the existence of a current wedge like that during substorms.

2.4. Waveform Comparison

[19] In this subsection, we continue to compare the waveforms of the four consecutive Pi2s in space to those at the
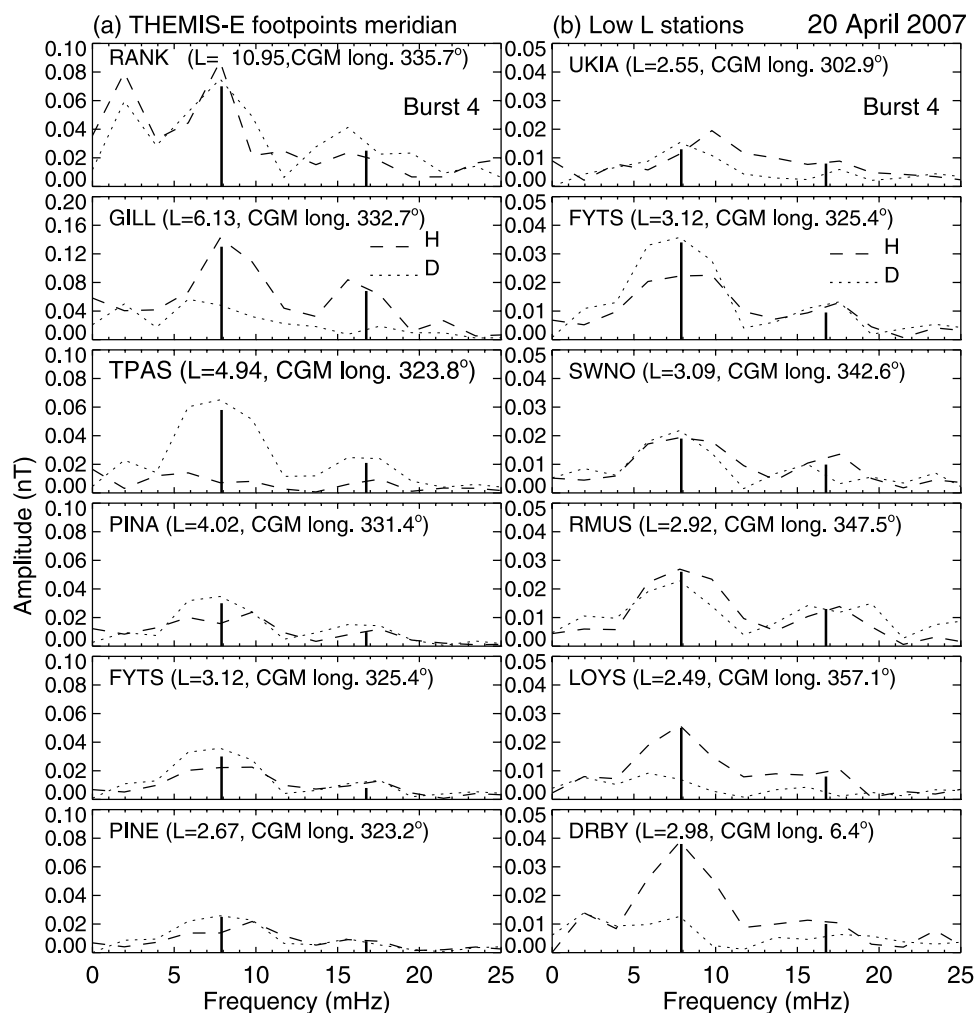
Figure 9. In the same format as Figure 7, except for burst 4.

ground stations to verify if their source waves are correlated with one another in the near-Earth magnetotail. Figure 13 shows the waveforms in the Bp component of four Pi2 bursts at THEMIS-E and those in the H component at the ground-based stations close to the THEMIS-E foot points meridian. The vertical dotted lines denote the most same peaks in the waveforms seen by the ground stations. For burst 1, the Pi2 wave at RANK leads those at THEMIS-E and other ground stations at the beginning of the first cycle. Later, the second and third wave cycles become in phase with one another. Burst 2 at THEMIS-E first lags behind that at RANK but leads other ground stations by ~90° in the first cycle. But for the rest cycles, burst 2 at THEMIS-E becomes in phase with that at RANK. Moreover, the H component at RANK is out of phase with those at other ground stations. As for burst 3, the waveform at THEMIS-E is not as clear as those on the ground stations. For the first peak, the waveform at THEMIS-E is in phase with those at low L stations but out of phase with those seen by RANK and GILL. For burst 4, the Pi2 wave at RANK leads those at THEMIS-E and other ground stations by ~90°. In particular, burst 4 at THEMIS-E is in phase with GILL but out of phase with those at low L stations. Figure 14 shows the waveforms in the H component of four Pi2 bursts at low L

stations in a longitudinal separation. FYTS is the closest to the THEMIS-E foot points. For bursts 1 and 3, the waveform is not strong but still in phase at most low L stations, except UKIA. In contrast to bursts 1 and 3, bursts 2 and 4 have strong waveforms and an in-phase relationship for most low L stations. The waveform at UKIA is not the same as other stations for bursts 1 and 3, and slightly ahead 90° in the last peak for bursts 2 and 4 as well. Hence, Figures 13 and 14 clearly verify that the fast compressional mode is the main source wave from the magnetotail for consecutive Pi2s in this event study. Especially for bursts 2 and 4 in Figure 13, the Bp and H components have the characteristics of the fundamental cavity mode resonance with 180° of phase change from high to low latitudes across the plasmapause [see *Lin et al.*, 1991; *Cheng et al.*, 1998, 2000].

[20]   In the same format as Figure 13, Figure 15 shows the waveforms in the Bn component at THEMIS-E and the D component at the ground-based stations close to the THEMIS-E foot points meridian. For burst 1, the Pi2 wave at THEMIS-E is slightly ahead 90° with those on the ground stations, except for being in phase with RANK for the first two peaks. As for burst 2, one finds that the Pi2 wave at RANK has the largest amplitude and leads others by ~90° throughout the duration time. For burst 3, the waveform at THEMIS-E is
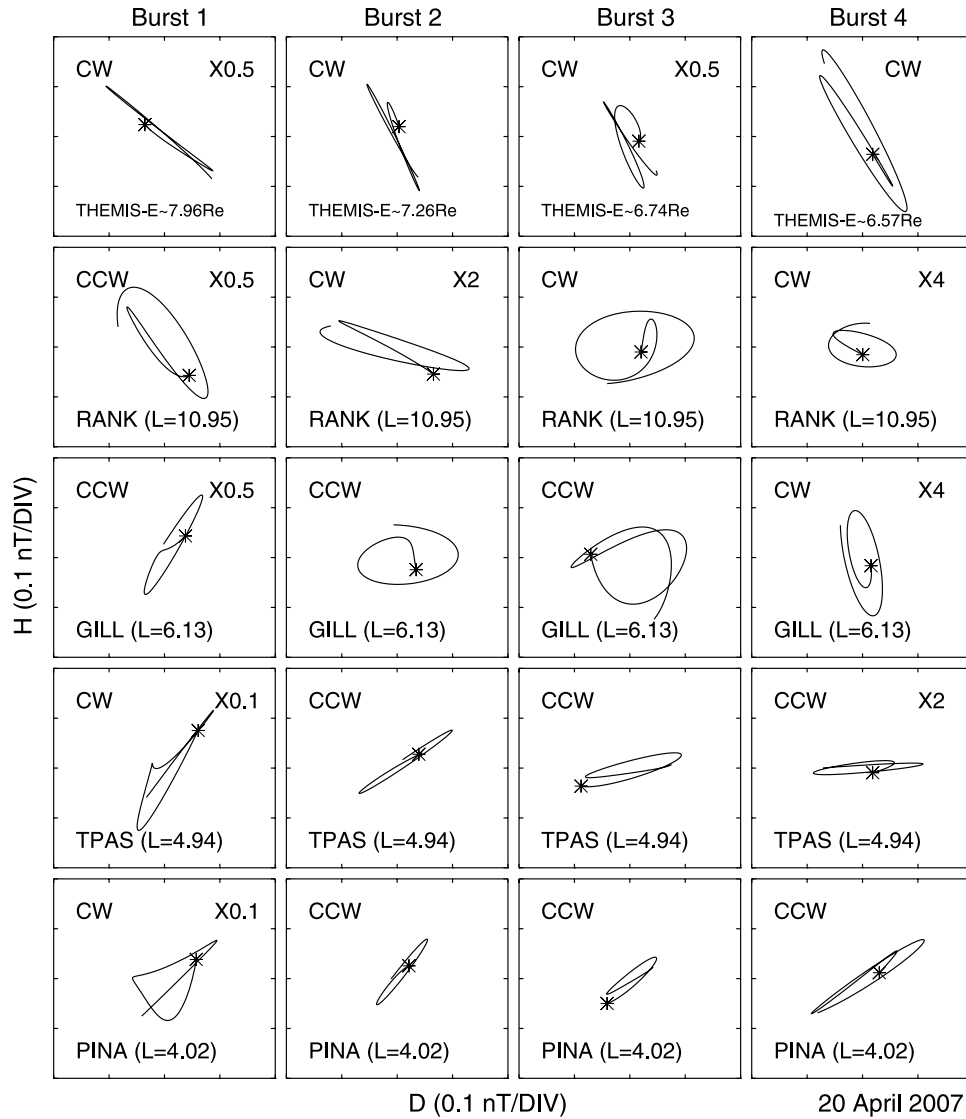
Figure 10. The hodogram of four Pi2 bursts at THEMIS-E and the ground stations close to the foot points. The asterisk denotes the starting point. CW and CCW denote clockwise and counterclockwise polarizations, respectively.

not clear, but those at most of the ground stations look in phase except for RANK leading by ∼90°. In the same way as burst 2, burst 4 at RANK has the largest amplitude fluctuation and leads others by ∼90° in the first two peaks. In contrast to bursts 1 and 3, bursts 2 and 4 have clear waveforms and in-phase relationship for most of the ground stations except RANK. In the same format as Figure 14, Figure 16 shows the waveforms in the *D* component at low *L* stations in a longitudinal separation. For burst 1, Pi2 wave fluctuations are weak but visible at FYTS and DRBY. For burst 3, the waveform at FYTS is strongest and the first peak appears in phase for all low *L* stations. Noteworthy, the second peak at DRBY leads LOYS by ∼15 s. LOYS also slightly leads other ground stations by a few seconds. Along with the same clear waveforms, the above phenomena can be found from bursts 2 and 4 as well. Figures 15 and 16 indicate that except for burst 1, the right wing of the substorm-like current wedge first forms east of the DRBY longitude, and

shortly the west wing appears along the longitude of the THEMIS-E foot points. These observations further verify that a substorm-like current wedge existed and expanded westward during the occurrence of the last three bursts, just like at the substorm expansion onset.

[21] Our analysis shows that the impulsive source responsible for the four consecutive Pi2 bursts must located at the longitude of THEMIS-E foot points. After onset, Pi2 waves propagate westward and eastward from the source longitude in the near-Earth magnetotail. These observational results are consistent with the findings of *Cheng et al.* [2004]. Thus, we suggest that these Pi2 bursts have the same generation and propagation mechanisms as those during substorm times.

3. Discussion

[22] In the review by *Baker et al.* [1996], substorm-related disturbances in the nightside near-Earth magneto-
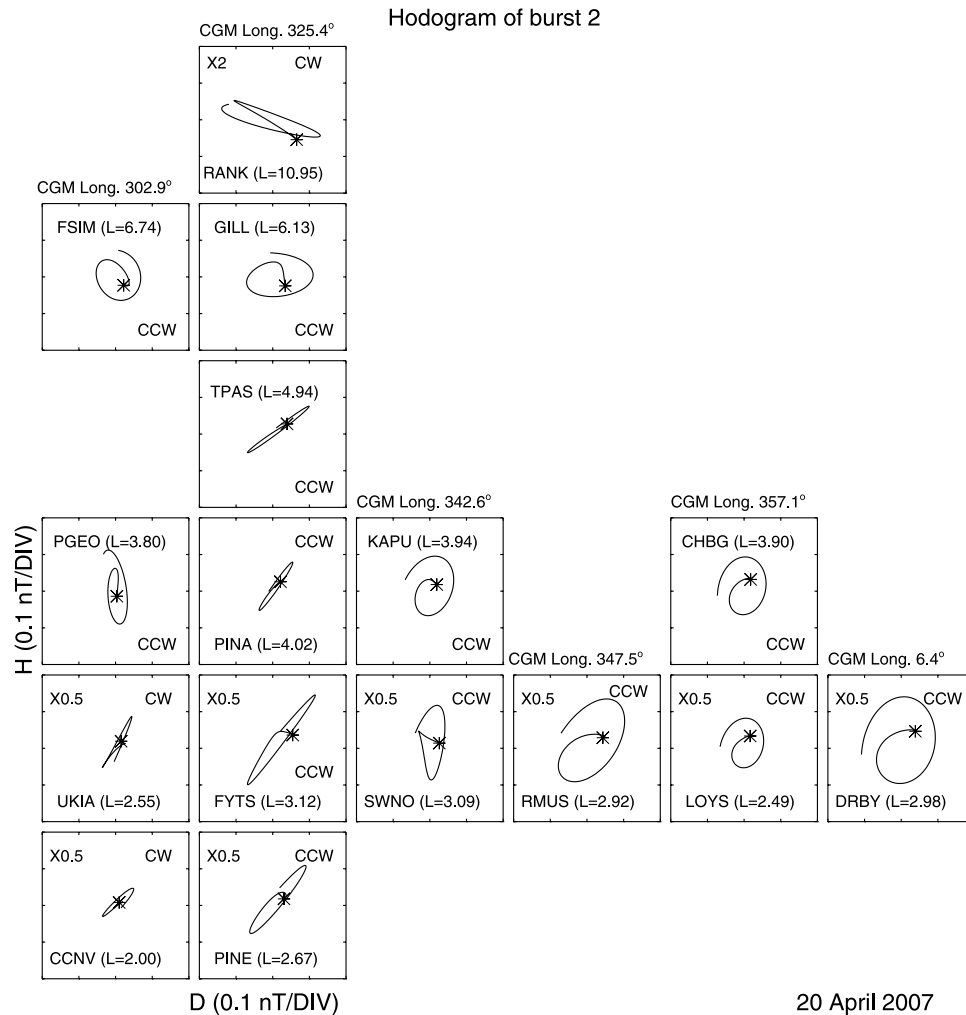
Figure 11. The hodogram of the burst 2 at the stations around the longitude close to the THEMIS-E foot points. The asterisk denotes the starting point. CW and CCW denote clockwise and counterclockwise polarizations, respectively.

sphere commonly include the formation of the current wedge, energetic particle injections, magnetic bays at high latitudes and Pi2 pulsations. In addition, these features can successively occur in a sequence [e.g., *Cheng et al.*, 2005]. As shown above, on 20 April 2007, four consecutive Pi2 bursts occurred simultaneously in the premidnight sector at the THEMIS-E probe and ground stations while the *AE* index was less than 100 nT (see Figure 3). Especially for the last three Pi2 onsets, ground stations and GOES 12 observed magnetic perturbations like the ones affected by the formation of the substorm-like current wedge. LANL 94 also detected an enhancement of energetic-particle flux (see Figures 4 and 5). In the introduction, we pointed out that it is still undetermined how substorm-related activations like Pi2s can successively appear in the quiet times. Namely, investigating the source mechanism of Pi2 pulsations occurring at times of weak geomagnetic activity is vital and needed for the determination of whether their cause and effect are different from those during substorm times.

[23] In earlier studies [e.g., *Samson and Harrold*, 1983, and references therein], the polarization pattern of Pi2 pulsations in the auroral region was considered to be dominantly controlled by the westward electrojet during substorm onsets. *Pashin et al.* [1982] proposed that the polarization reversal can occur through a westward movement of the upward field-aligned current, linking the westward electrojet to the cross-tail current in the plasma sheet. In the review and outlook by *Baumjohann and Glassmeier* [1984], Pi2 pulsations at high latitudes are the transient responses within the Earth's magnetosphere during substorm onsets and can be interpreted as part of the signature of the substorm current system. However, *Lester et al.* [1985] found that high-latitude Pi2 pulsations can be associated with the eastward electrojet and governed by the field line resonance mechanism while away from the auroral breakup region. Later, based on the polarization patterns and the orientation of the major axis, the formation of the current wedge has been suggested to be responsible for midlatitude and low-latitude Pi2 pulsations during substorms [e.g., *Lanzerotti and Medford*, 1984; *Lester et al.*, 1989, and references therein]. For the 20 April 2007 event, we performed a hodogram analysis on four consecutive Pi2s in space and on the ground. The hodogram analysis shows that the direction of the major axis orients toward the
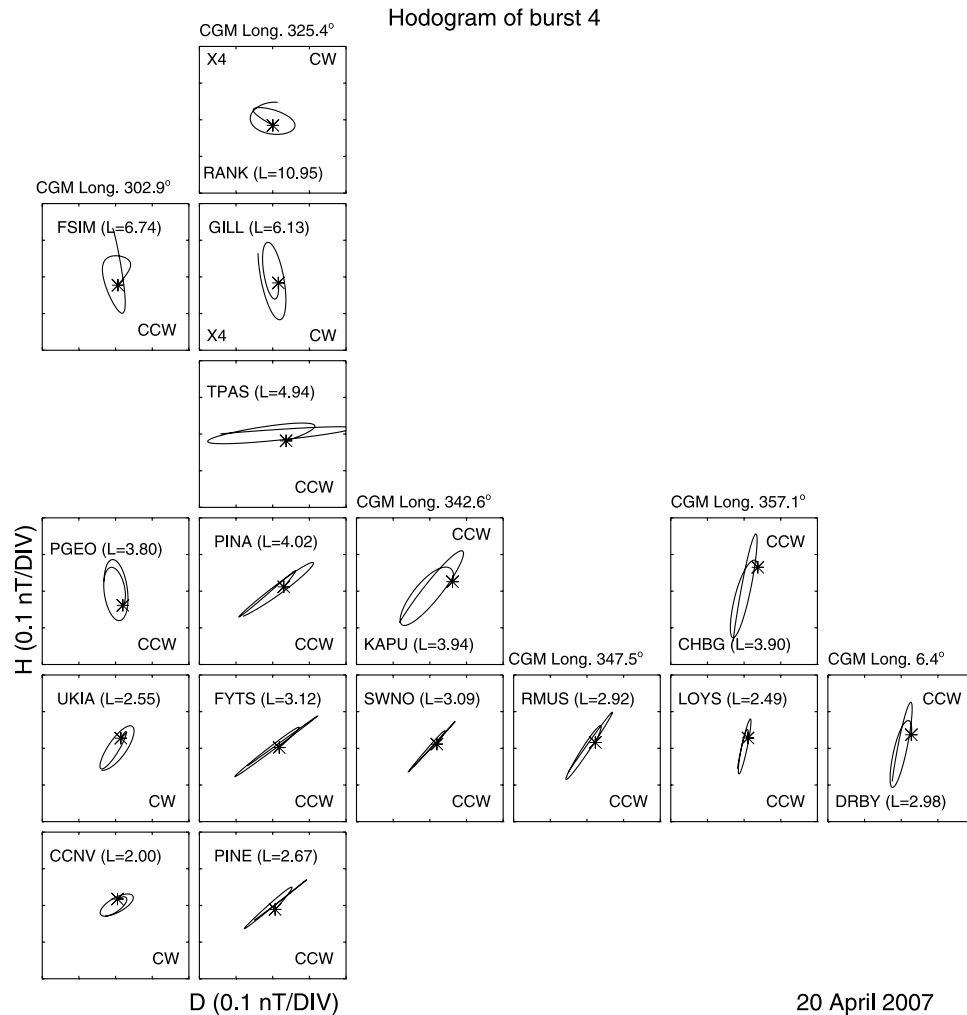
Figure 12. In the same format as Figure 11, except for burst 4.

location of the current wedge center as it does during substorms (see Figures 10–12). This inference is verified with the perturbations of the D component at the ground stations like those affected by the upward field-aligned current in the west wing of the substorm-like current wedge (see Figures 4b, 15, and 16). To further justify the above inference, we have plotted the horizontal magnetic variation vectors consisting of H and D components, removed from their 12 min running means, sensed by the ground stations around the THEMIS-E foot points to simulate the equivalent current vector like those adopted by *Untiedt and Baumjohann* [1993]. Figure 17 shows the horizontal magnetic variation vectors in the coordinates of L value versus corrected geomagnetic longitude at each Pi2 onset. The black circles denote the locations of the ground stations. One can see from Figure 17 that there are four magnetic vortex patterns of which the first looks like the one affected by the downward field-aligned current and the three others by the upward field-aligned current. Noteworthy, the vectors at the $L \sim 6$ (corresponding to GILL) station appear to be much more prominent than those at other stations. By checking out Polar UVI images (not shown in this study) in the online archives, we find that auroral activations occurred around geomagnetic latitude $70°$ (corresponding to $L \sim 6$)

during the time of interest that is the reason for the prominent vectors at GILL. The wave polarizations at the ground stations in the wide longitude span around $L \sim 3-4$ appear to be CCW (see Figures 11 and 12). These results are the same as in Figure 1 of the *Lester et al.* [1984] study. Hence, for this event, it is likely that the formation of the current wedge can occur in the same way as those at substorm onsets.

[24] According to *Shiokawa et al.* [1998], the braking of bursty bulk flows (BBFs) may be responsible for the upward field-aligned current and the forming of the substorm current wedge by the closure of the westward electrojet in the auroral ionosphere. Compared to other stations along the meridian of THEMIS-E foot points, the H component of the magnetic field at GILL has a magnetic bay after each Pi2 onset (see Figure 4a). Except for burst 1, the D component is enhanced from high to low latitudes after the last three onsets (see Figure 4b). For bursts 2 and 3, the polarization changes from CW to CCW in between RANK and GILL. The polarization reversal occurs in the middle of GILL and TPAS for burst 4. These imply that the westward electrojet may be located around GILL, and the field-aligned current may be upward over GILL as well. Moreover, in Figures 5a and 5c, magnetic field perturba-
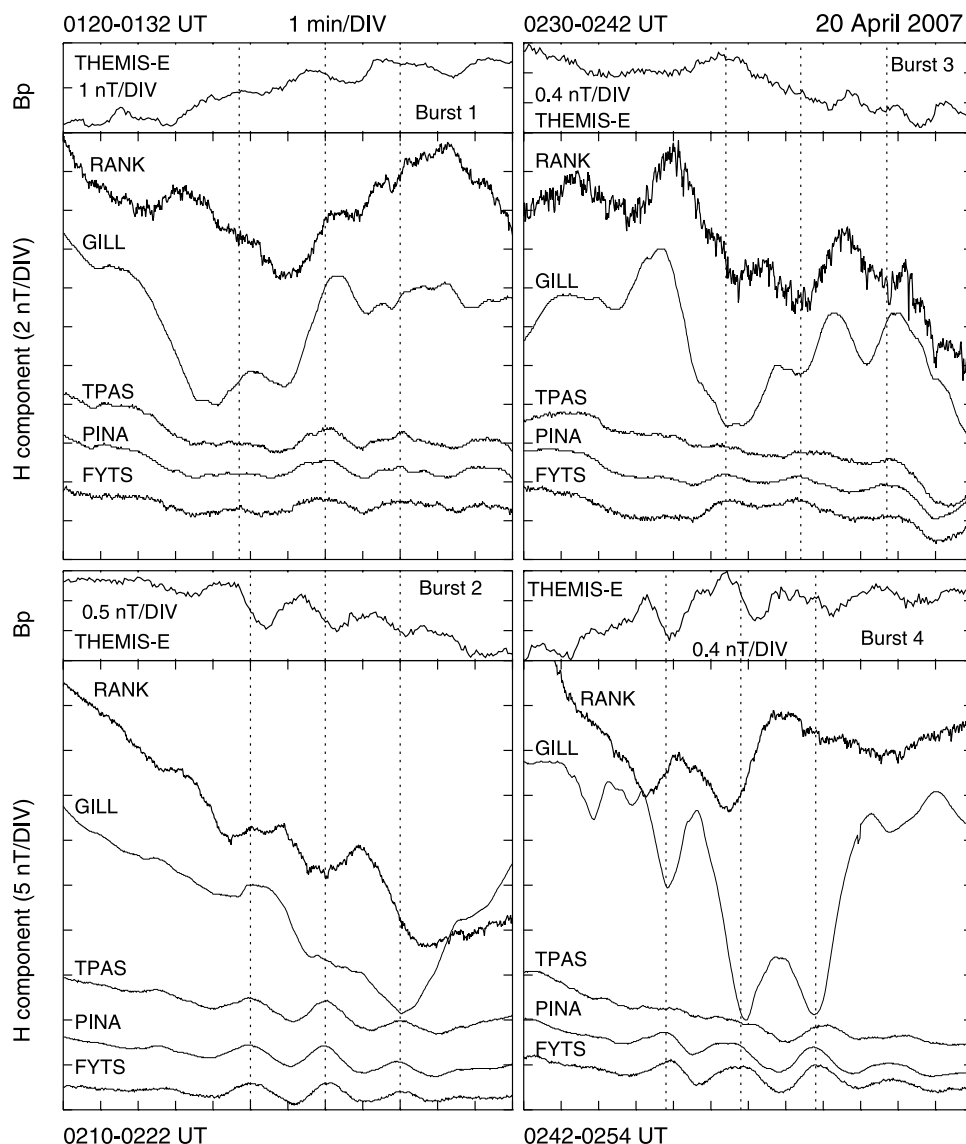
Figure 13. The waveforms in the *Bp* component of four Pi2 bursts at THEMIS-E and those in the *H* component at the ground-based stations close to the THEMIS-E foot points meridian. The vertical dotted lines denote the most same peaks in the waveforms seen by the ground stations.

tions at GOES 12 show that the *Hp* component has positive perturbations and that the *He* component has wave-like perturbations after the second, third and fourth Pi2 onsets. Moreover, LANL 94 observed the enhanced energetic electron flux after the last three Pi2 onsets. These signify the formation of the substorm-like current wedge during the time of interest. Hence, the BBF model can be a plausible generation scenario for the last three Pi2 bursts.

[25] After onset, earthward BBFs may brake in the near-Earth magnetotail due to the balance of magnetic pressure and flow kinetic pressure. As a result, at least two kinds of hydromagnetic waves are driven impulsively by earthward BBFs. One is a fast compressional wave, propagating from the BBF braking region and bouncing back from the Earth. During the lifetime of earthward BBFs, fast compressional waves are trapped in the inner magnetospheric cavity and result in a cavity resonance [e.g., *Cheng et al.*, 2000, and references therein]. In this study, Figures 6–9 show that

four consecutive Pi2 bursts have the matched frequency ~6–8 mHz between THEMIS-E and the ground stations. Moreover, there is another harmonic frequency ~17 mHz for burst 4. The waveform comparisons shown in Figures 13 and 14 further verify that the cavity resonance mode can play a dominant role in the four consecutive Pi2 bursts observed by the THEMIS mission, in addition to the formation of the substorm-like current wedge.

[26] From Figure 6, one can see that the dominant frequency, ~6.5 mHz, of burst 1 at THEMIS-E is smaller than the others with ~8 mHz. If a fast magnetospheric cavity resonance mode is excited by the impulsive source in the magnetotail after onset, its eigen frequency should be determined by the size and structure of the resonant cavity. After the first onset, the geomagnetic configuration becomes more dipolarized like the one during substorms. The outer boundary of the inner magnetospheric cavity for the other bursts would move earthward more than that for
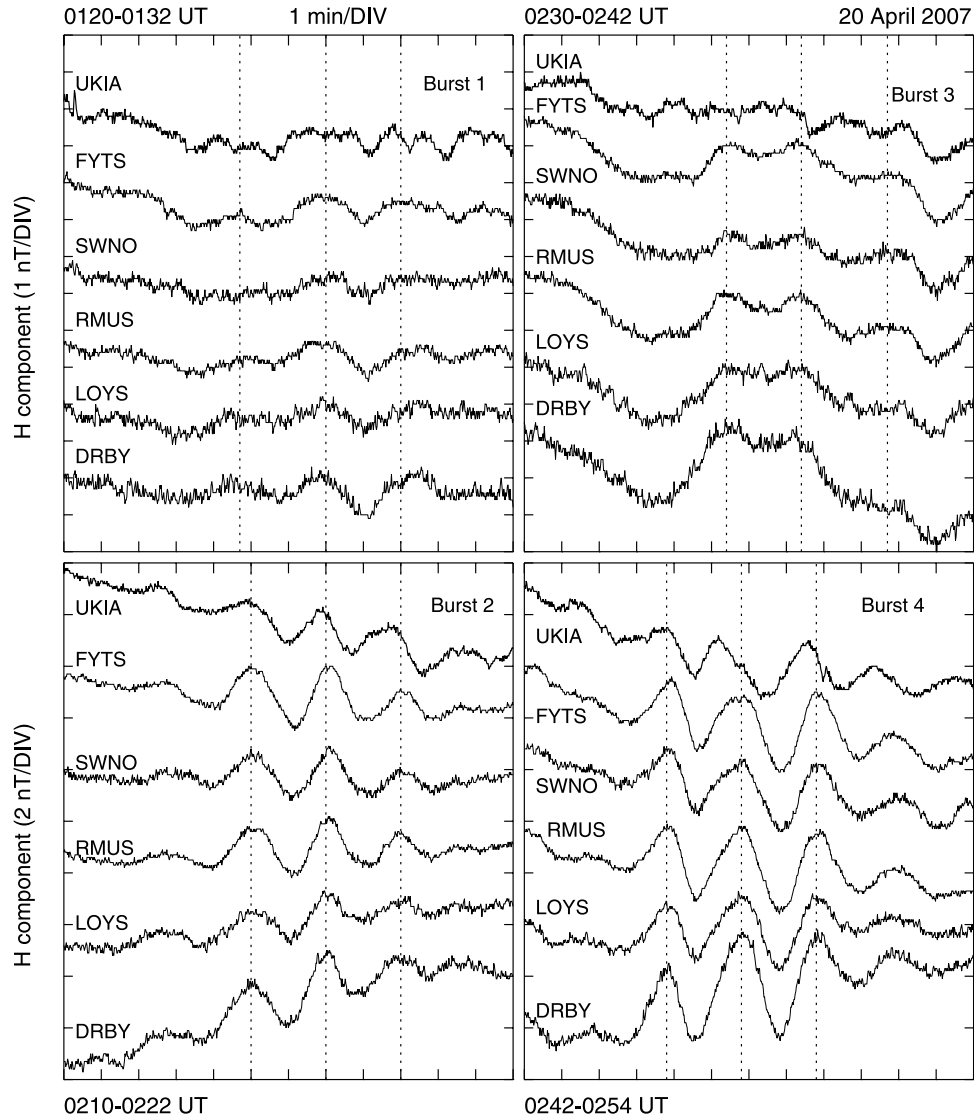
Figure 14. In the same format as Figure 13, except for the low *L* stations. FYTS is the closest station to the THEMIS-E foot points.

the first one. Therefore, the dominant frequency of the other bursts would become higher than the first one. As for another harmonic frequency, $\sim$17 mHz, of burst 4 shown in Figure 6, it may be the plasmaspheric cavity resonance mode. On the basis of the same waveforms and no phase delays between the multipoint ground and satellite observations, *Nosé et al.* [2003] suggested that low-latitude Pi2s during a geomagnetic quiet period could extend to the morning side and might result from the plasmaspheric cavity resonance mode. Burst 4 has a slightly larger dominant frequency than burst 2 (see Figure 6). Figure 13 indicates that the impulsive source gets closer to the plasmapause for burst 4 than burst 2. The fast compressional wave could then be trapped in the inner magnetosphere, as well as in the plasmasphere. If earthward BBFs spread in a wide longitudinal extent, the strength of the magnetospheric cavity resonance mode would be stronger than the plasmaspheric cavity resonance mode. This is the reason why the spectral amplitude of the second peak frequency is smaller than the first peak frequency (see Figures 7 and 9). This also

explains why the amplitudes of bursts 2 and 4 tend to decrease eastward and westward from the meridian of the THEMIS-E foot points in the premidnight sector (see Figure 16). A similar trend can be found in Figure 3 of the *Nosé et al.* [2003] study except from the postmidnight to the morning.

[27] There is another view about the generation of mid and low Pi2 pulsations that shear Alfvén waves in a localized field line oscillation inside the plasmapause result from the coupling of the fast magnetospheric cavity resonance mode to field line resonances as their eigen frequency matches. In Figures 3 and 13, the amplitude enhancement and phase change of bursts 3 and 4 at GILL is similar to those studied by *Cheng et al.* [1998], due to the coupling of a fast magnetospheric cavity resonance mode to field line resonances in the inner magnetosphere. Especially for burst 3, the ground stations have the same spectral peak at $\sim$8 mHz, and there is another spectral peak at $\sim$12 mHz only seen at GILL (see Figure 8). Moreover in Figure 15, the wave fluctuation in the *Bn* component at THEMIS-E is
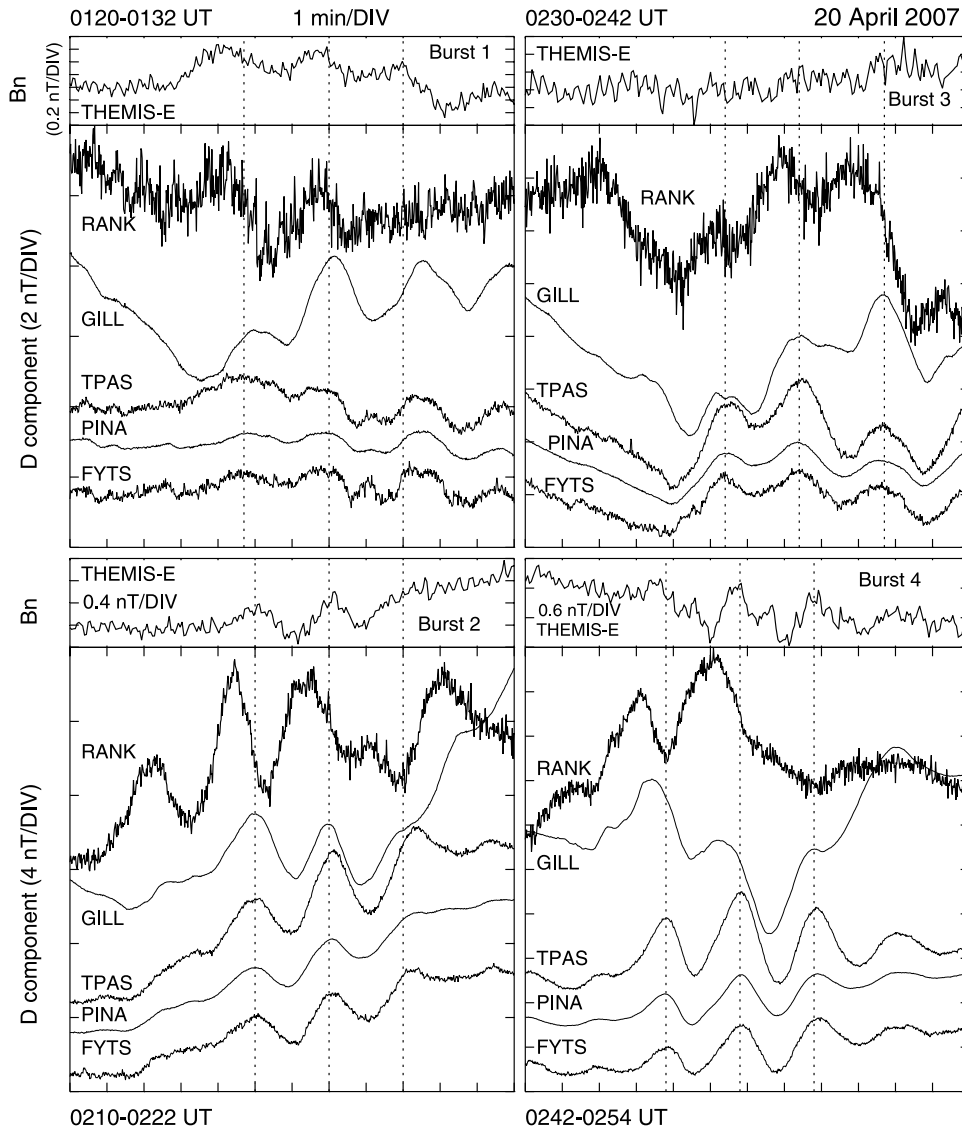
Figure 15. In the same format as Figure 13, except for the *Bn* component at THEMIS-E and the *D* component at the ground-based stations.

not clear like the node feature of the fundamental mode of a localized field line oscillation. Since GILL was close to the THEMIS-E foot points, bursts 3 and 4 can be composed of the shear Alfvén wave and the fast magnetospheric cavity resonance mode. By analyzing the latitudinal profile of the peak power of Pi2 pulsations in the Circum-pan Pacific Magnetometer Network (CPMN), *Yumoto and the CPMN Group* [2001] found that the peak power of *H* and *D* components of Pi2 pulsations becomes interchanged from high to low frequency at stations close to plasmapause. In Figures 7–9, the power spectrum at GILL close to the plasmapause foot points has the same features as *Yumoto and the CPMN Group* [2001] suggested. Moreover, braking BBFs may stimulate the surface wave at the plasmapause with a steep gradient in Alfvén speed. *Kosaka et al.* [2002] reported that the dominant frequency of midlatitude Pi2 is consistent with the resonance frequency of the surface wave at the plasmapause in a plasmaspheric model including the effect of plasmapause bulge. In this study, however, the Pi2

amplitude of the last three bursts does not have a strong latitudinal decline from TPAS (*L* = 4.94) just inside the plasmapause down to low *L* stations (see Figures 13 and 15). In contrast, the cavity resonance mode is more dominant in the inner magnetosphere than the surface wave excited at the plasmapause.

[28] In addition to BBFs, current disruption in the magnetotail is the other impulsive source associated with geomagnetic reconfiguration after substorm onset. Assuming the impulsive source current as a wave generator in the magnetotail, *Fujita et al.* [2002] and *Fujita and Itonaga* [2003] simulated the behavior of hydromagnetic waves in a model magnetosphere with a longitudinally nonuniform plasmasphere after substorm onset. Their simulation results show that the major axis of polarization of magnetic perturbations, like Pi2s, are radially oriented at midnight and azimuthally oriented at dawn and dusk. They also found that the cavity resonance mode in a Pi2 period could be sustained in the plasmasphere and the field line resonance
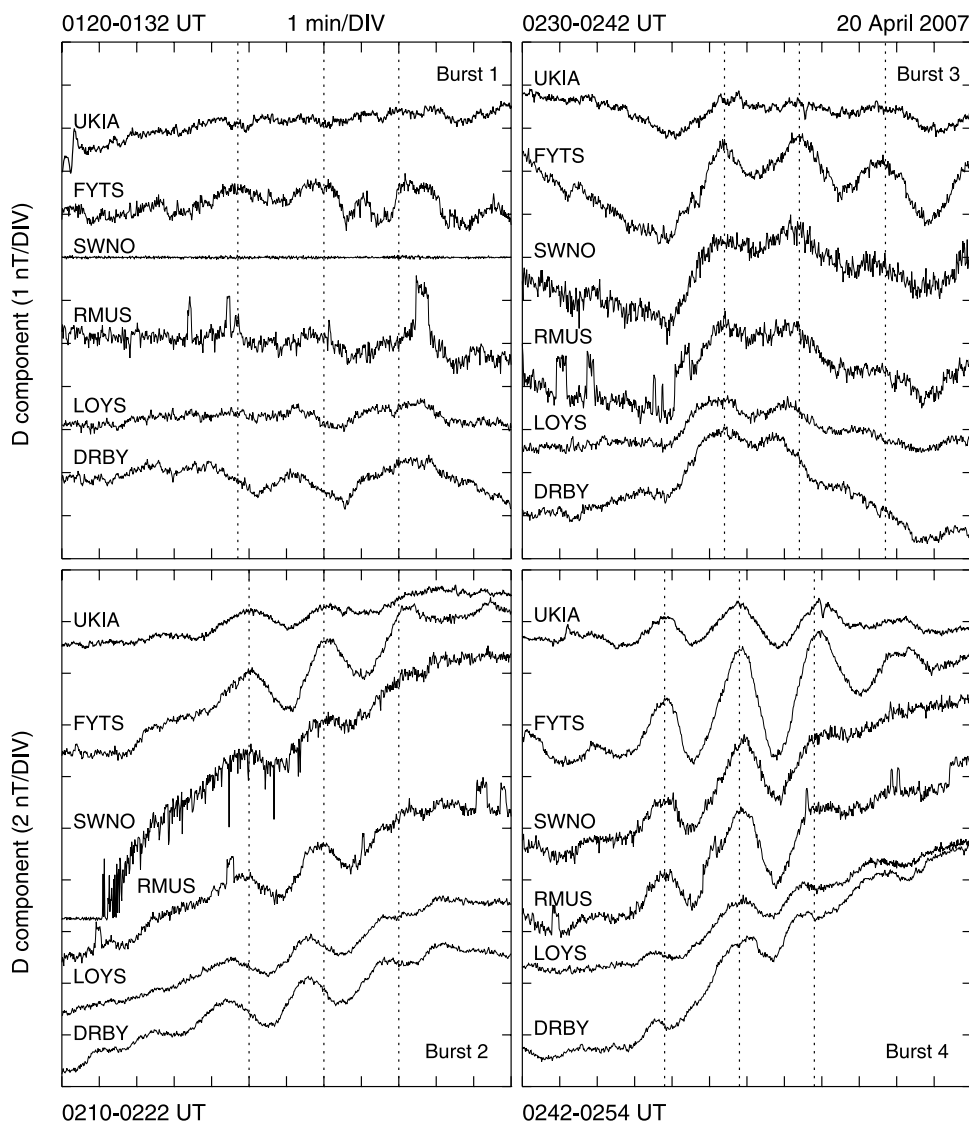
Figure 16. In the same format as Figure 14, except for the *D* component.

could be excited in regions with a steep gradient of Alfvén speed as well. Further, the plasmaspheric cavity resonance mode could have local time dependent spectra like those observed by the ground stations. In addition, the localized field line resonance mode could have the same tendency of local time dependent spectra as the plasmaspheric cavity resonance mode. Unlike the cavity mode, the surface wave is an evanescent fast mode, and its amplitude decreases as it propagates isotropically. *Fujita and Itonaga* [2003] suggested that the surface wave could be a possible generation mechanism for Pi2s localized in a longitudinal direction. This may be the reason why the amplitude of low-latitude Pi2s tends to decrease eastward and westward from the meridian of the THEMIS-E foot points in the premidnight sector (see Figure 16). The simulation features by *Fujita et al.* [2002] and *Fujita and Itonaga* [2003] are qualitatively consistent with our observational results. Hence, we cannot rule out the possibility that current disruption may be another source candidate for the last three Pi2 bursts.

[29] In order to ascertain which model is more viable for this event, we have scanned the magnetotail observations on 20 April 2007. Unfortunately, there were only strong tailward BBFs detected by Geotail at $Xgse \sim -25\ Re$ prior to each ground Pi2 onset (not shown in this study). Despite no direct evidence for earthward BBFs, the magnetic fields sensed by Geotail do not have the signature of tailward movement of dipolarization such as might be caused by the near-Earth current disruption either. Since magnetotail reconnection can launch both earthward and tailward BBFs, the BBF model is more plausible for this event than current disruption. One may argue that Geotail at $Xgse \sim -25\ Re$ seems far from the near-Earth substorm onset site. To explain the double-onset observations [e.g., *Mishin et al.*, 2001], *Russell* [2000] extended the near-Earth neutral point model by *Russell and McPherron* [1973], with emphasis on the role of the distant neutral point. In the model, the interplay between near-Earth and distant neutral points in the magnetotail creates two onsets, one when reconnection at the near-Earth neutral point first begins on closed field lines within the plasma sheet, and one when the near-Earth neutral point reaches the open flux of the tail lobes. The timing of the second onset is controlled by the distant
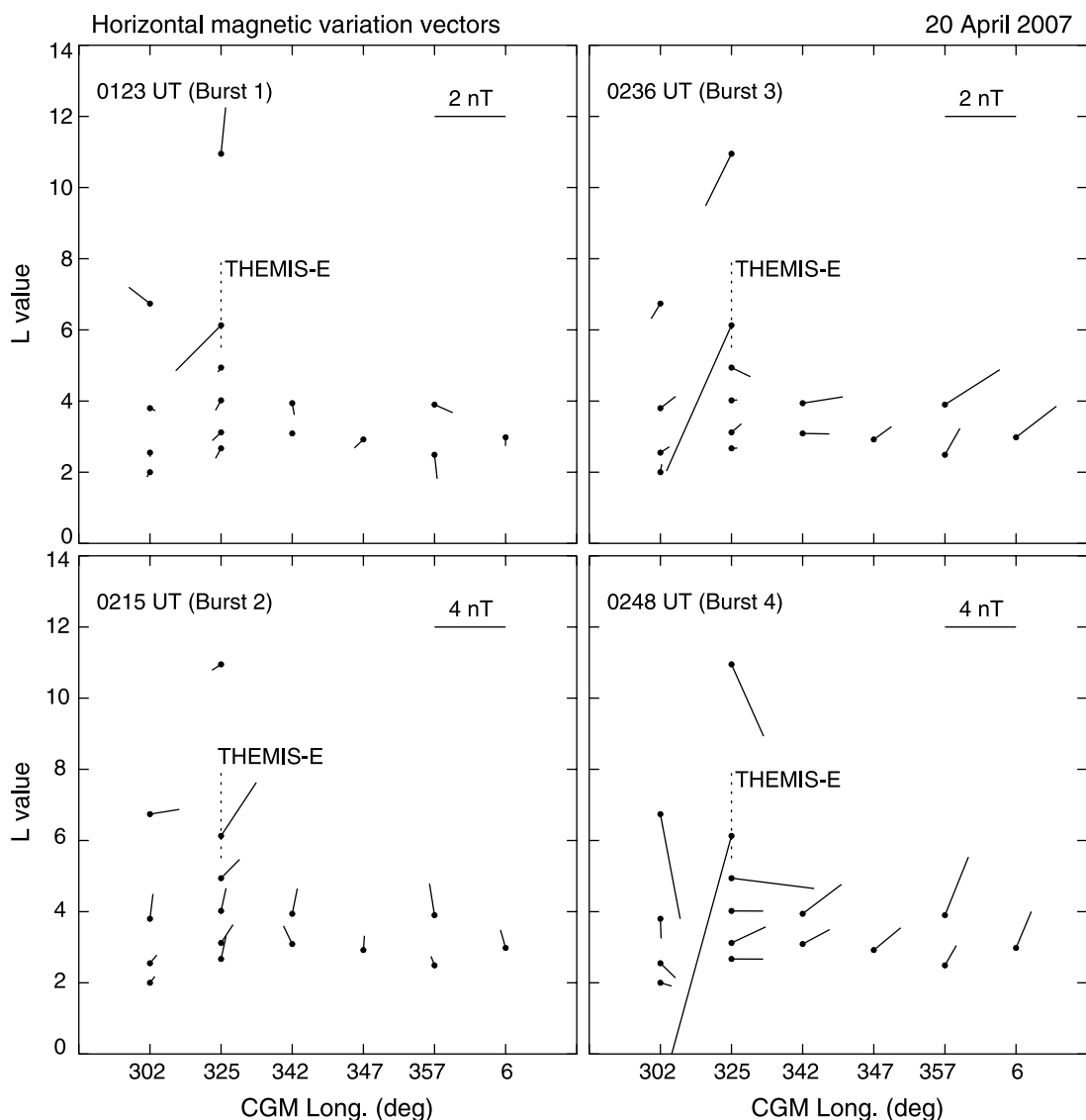
Figure 17. The horizontal magnetic variation vectors consisting of *H* and *D* components sensed by the ground stations around the THEMIS-E foot points (the vertical dotted lines) at each Pi2 onset. The black circles denote the locations of the ground stations.

neutral point that, in turn, is controlled by northward turning of the IMF. To further verify if four consecutive Pi2 onsets are externally triggered, we have also looked at the IMF observations just in front of the Earth's magnetopause. Figure 18 shows the IMF variation sensed by Cluster at *Xgse* ∼ 10.0 Re and by the satellite in the upstream region shifted to the location of the Earth. Except for the first onset with northward turning at 1 AU (corresponding to *Xgse* ∼ 17.0 *Re*) only, three other onsets are associated with northward turning at both locations. Note that bursts 3 and 4 onsets are so close in a series that they can be regarded as the kind of double-onset substorms reported by *Cheng et al.* [2005]. Hence, as *Cheng et al.* [2009] suggested, the two-neutral-point model can explain why four Pi2 bursts occur successively in addition to the BBF model for their source mechanisms.

[30] According to *Itonaga and Yumoto* [1998], low-latitude Pi2 waves can propagate eastward with the CW polarization, and westward with the CCW polarization from the source longitude. In Figures 11 and 12, Pi2 waves appear CCW polarized at FTYS and PINE and turn to be CW polarized at UKIA and CCNV. This low-latitude polarization reversal in the east and west of the source longitude is contrary to the suggestion by *Itonaga and Yumoto* [1998]. Note that their suggestion is based on two conditions that the phase of the *H* component is latitudinally constant, and the *D* component is 180 degrees out of the phase to the east and west of the source longitude. The latter condition is not met by the low-latitude *D* component on 20 April 2007, with the same phase longitudinally (see Figure 16). Thus, more event studies are needed in the future to find out whether this different polarization reversal is casual or common. For the last three onsets in this study, however, the longitudinal Pi2 wave distributions shown in Figures 14 and 16 are consistent with the observational result reported by *Yumoto and the CPMN Group* [2001]: that Pi2 in the premidnight sector occurs earlier than that in the evening
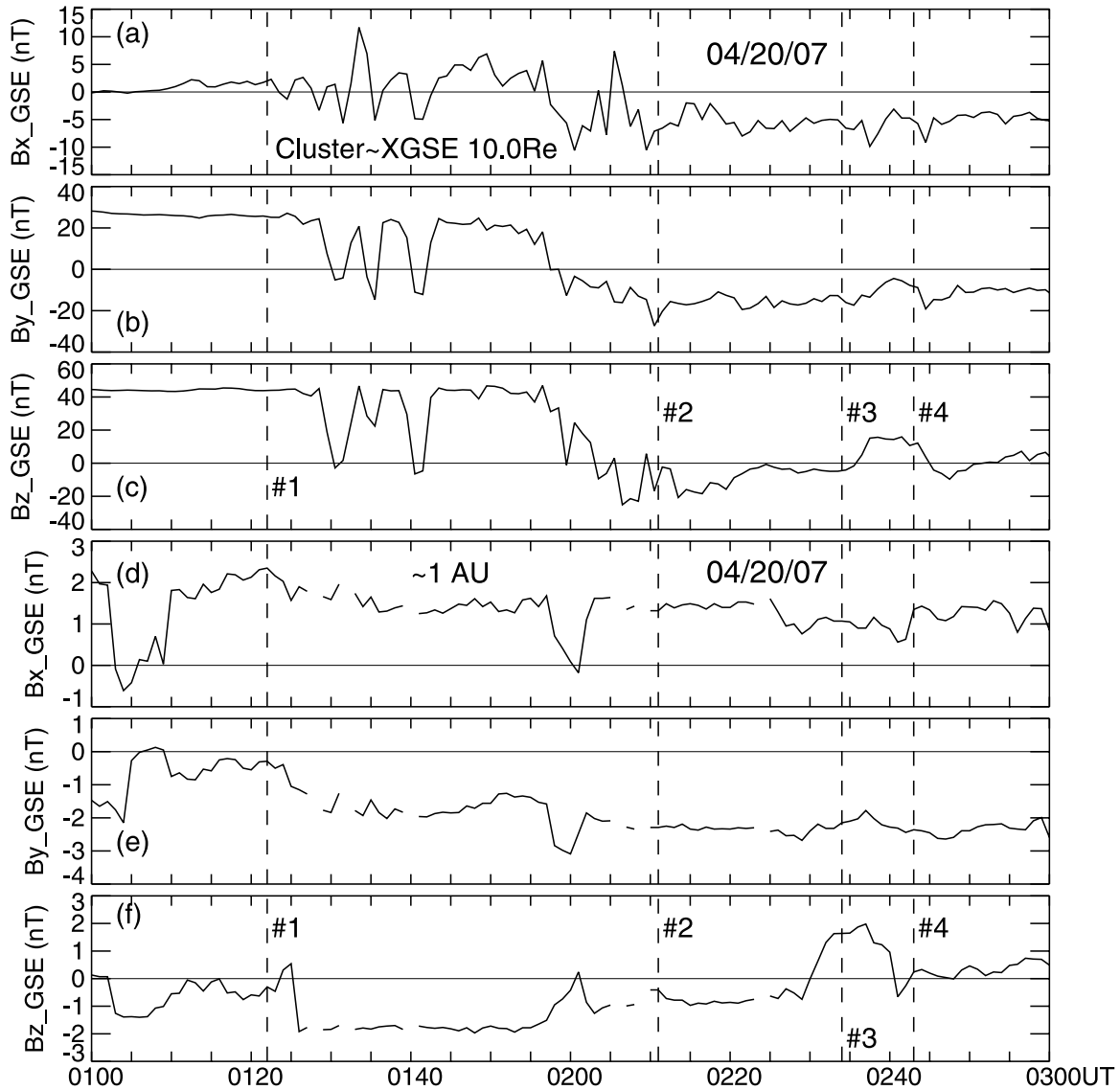
Figure 18. The three components of the IMF in GSE coordinates sensed by (a–c) Cluster at $Xgse \sim 10.0\,Re$ and (d–f) the satellite in the upstream region shifted to 1 AU (corresponding to $Xgse \sim 17.0\,Re$).

sector. As a result, Pi2s near the source site can be composed of at least three components, including the substorm-like current wedge oscillation, the surface wave at the plasmapause or a localized field line oscillation inside the plasmapause, and the magnetospheric/plasmaspheric cavity resonance mode. But away from the source longitude, the substorm-like current wedge oscillation and the cavity resonance mode are the main components for nighttime Pi2s.

[31] Except for the substorm-like current wedge, other factors responsible for consecutive Pi2s in this study are closely associated with the plasmapause location. The plasmasphere shape changing with time may lead to the local time dependence of the dominant frequency of low-latitude Pi2s. Recent imaging measurements at the spacecraft [e.g., *Burch et al.*, 2001] showed that the plasmasphere rarely had a smooth steady shape, and sometimes even had a plasma tail in the dusk sector. The asymmetric plasmasphere may not vary uniformly so that the difference of the

plasmapause distance might be mainly a temporal effect. Therefore, the temporal variation of the plasmapause location may result in a slight frequency difference of midlatitude and low-latitude Pi2s at different longitudes. This is the reason why the dominant frequency at the low L stations cannot be exact as that seen at THEMIS-E. Nonetheless, the latitudinal and longitudinal dependences of the dominant frequency and polarization characteristics of the last three Pi2 bursts on 20 April 2007 are the same as those during substorm times.

[32] Finally thanks to the magnetometers with magnetic sensitivity better than 0.1 nT set up by the THEMIS mission, we are able to retrieve the observations of small-amplitude Pi2 pulsations simultaneously occurring in space and on the ground. In this study, Figure 15 shows a unique example of THEMIS-E Pi2s with very small amplitude less than 0.1 nT having one-to-one correspondence with those on the ground stations in a weak geomagnetic period, hereby an unprecedented finding to study what is the exact

source mechanism for quiet time Pi2s. Namely, this study shows the fact that quiet time Pi2s and small substorms can be just as associated as large ones are and the improvement in the resolution relative to previous missions results in a better correlation between ground and space phenomena.

4. Summary and Conclusions

[33] On 20 April 2007, four Pi2 pulsation bursts occurred successively and simultaneously in the premidnight at the E spacecraft and the ground-based observatory system for the THEMIS mission, while the *AE* index was less than 100 nT.

[34] Except for the first onset, ground-based magnetometers and GOES 12 sensed magnetic perturbations like the one affected by the formation of the substorm-like current wedge. Moreover, LANL 1994–084 detected the enhancement of energetic particle flux.

[35] Spectral analysis shows a matched wave frequency of ~6–8 mHz for all Pi2 bursts and another harmonic frequency of ~17 mHz for burst 4. The hodogram shows an orientation of the major axis of the wave polarization toward the location of the substorm-like current wedge. The first burst has both latitudinal and longitudinal polarization changes from counterclockwise to clockwise, compared with three others with opposite latitudinal reversals only. The longitudinal clockwise to counterclockwise change at low latitudes signifies that hydromagnetic waves propagate westward and eastward from the longitude of the impulsive source responsible for the substorm-like current wedge. The latitudinal clockwise to counterclockwise reversal looks like the one induced by a westward moving upward field-aligned current carried by Alfvén waves leading to field line oscillations.

[36] As a result, the generation and propagation mechanisms of these Pi2 bursts can be the coupling of a fast magnetospheric cavity mode driven by fast compressional waves to field line resonances as expected from braking of BBFs initiated by magnetotail reconnection externally triggered by northward tuning of the IMF. The 20 April 2007 event thus manifests that the source mechanism of consecutive Pi2s in a weak geomagnetic period can be the same as that during substorm times.

References

Angelopoulos, V. (2008), The THEMIS mission, *Space Sci. Rev.*, 141, doi:10.1007/s11214-008-9336-1.

Auster, H. U., et al. (2008), The THEMIS fluxgate magnetometer, *Space Sci. Rev.*, 141, doi:10.1007/s11214-008-9365-9.

Baker, D. N., T. I. Pulkkinen, V. Angelopoulos, W. Baumjohann, and R. L. McPherron (1996), Neutral line model of substorms: Past results and present view, *J. Geophys. Res.*, 101, 12,975–13,010.

Baumjohann, W., and K. H. Glassmeier (1984), The transient response mechanism and Pi2 pulsations at substorm onset - Review and outlook, *Planet. Space Sci.*, 32, 1361–1370.

Burch, J., et al. (2001), Global dynamics of the plasmasphere and ring current during magnetic storms, *Geophys. Res. Lett.*, 28, 1159–1162.

Cheng, C.-C., J.-K. Chao, and T.-S. Hsu (1998), Evidence of the coupling of a fast magnetospheric cavity mode to field line resonances, *Earth Planets Space*, 50, 683–697.

Cheng, C.-C., J.-K. Chao, and K. Yumoto (2000), Spectral power of low-latitude Pi2 pulsations at 210° magnetic meridian stations and plasmaspheric cavity resonances, *Earth Planets Space*, 52, 615–627.

Cheng, C.-C., C. T. Russell, Y. F. Gao, and P. J. Chi (2002a), On consecutive bursts of low-latitude Pi2 pulsations, *J. Atmos. Sol. Terr. Phys.*, 64, 1809–1821.

Cheng, C.-C., C. T. Russell, M. Connors, and P. J. Chi (2002b), Relationship between multiple substorm onsets and the IMF: A case study, *J. Geophys. Res.*, 107(A10), 1289, doi:10.1029/2001JA007553.

Cheng, C.-C., C. T. Russell, K. Yumoto, Y. F. Gao, and P. J. Chi (2004), Characteristics of consecutive bursts of Pi2 pulsations observed at the SMALL array: A new implication, *Earth Planets Space*, 56, 531–545.

Cheng, C.-C., C. T. Russell, G. D. Reeves, M. Connors, and M. B. Moldwin (2005), On the relationship between double-onset substorm, pseudobreakup, and IMF variation: The 4 September 1999 event, *J. Geophys. Res.*, 110, A07201, doi:10.1029/2004JA010778.

Cheng, C.-C., C. T. Russell, and J.-H. Shue (2009), On the association of quiet-time Pi2 pulsations with IMF variations, *J. Adv. Space Res.*, 43, 1118–1129, doi:10.1016/j.asr.2008.12.001.

Clauer, C. R., and R. L. McPherron (1974), Mapping the local time-universal time development of magnetospheric substorms using midlatitude magnetic observations, *J. Geophys. Res.*, 79, 2811–2820.

Fujita, S., and M. Itonaga (2003), A plasmaspheric cavity resonance in a longitudinally non-uniform plasmasphere, *Earth Planets Space*, 55, 219–222.

Fujita, S., H. Nakata, M. Itonaga, A. Yoshikawa, and T. Mizuta (2002), A numerical simulation of the Pi2 pulsations associated with the substorm current wedge, *J. Geophys. Res.*, 107(A3), 1034, doi:10.1029/2001JA900137.

Fukunishi, H. (1975), Polarization changes of geomagnetic Pi2 pulsations associated with the plasmapause, *J. Geophys. Res.*, 80, 98–110.

Hughes, W. J., and D. J. Southwood (1976), The screening of micropulsation signals by the atmosphere and ionosphere, *J. Geophys. Res.*, 81, 3234–3240.

Itonaga, M., and K. Yumoto (1998), ULF waves and the ground magnetic field, *J. Geophys. Res.*, 103, 9285–9291.

Kivelson, M. G., and C. T. Russell (1995), Geophysical coordinate transformation, in *Introduction to Space Physics*, edited by M. G. Kivelson and C. T. Russell, pp. 539–540, Cambridge Univ. Press, New York.

Kosaka, K., T. Iyemori, M. Nosé, M. Bitterly, and J. Bitterly (2002), Local time dependence of the dominant frequency of Pi2 pulsations at mid- and low-latitudes, *Earth Planets Space*, 54, 771–781.

Lanzerotti, L. J., and L. V. Medford (1984), Local night, impulsive (Pi2-type) hydromagnetic wave polarization at low latitudes, *Planet. Space Sci.*, 32, 135–142.

Lester, M., W. J. Hughes, and H. J. Singer (1984), Longitudinal structure in Pi2 pulsations and the substorm current wedge, *J. Geophys. Res.*, 89, 5489–5494.

Lester, M., K. H. Glassmeier, and J. Behrens (1985), Pi2 pulsations and the eastward electroject current: A case study, *Planet. Space Sci.*, 33, 223–233.

Lester, M., H. J. Singer, D. P. Smits, and W. J. Hughes (1989), Pi2 pulsations and the substorm current wedge: Low-latitude polarization, *J. Geophys. Res.*, 94, 17,133–17,141.

Lin, C. A., L. C. Lee, and Y. J. Sun (1991), Observations of Pi2 pulsations at a very low latitude (L = 1.06) station and magnetospheric cavity resonances, *J. Geophys. Res.*, 96, 21,105–21,114.

Mishin, V. M., T. Saifudinova, A. Bazarzhapov, C. T. Russell, W. Baumjohann, B. Nakamura, and M. Kubyshkina (2001), Two distinct substorm onsets, *J. Geophys. Res.*, 106, 13,105–13,118.

Nosé, M., et al. (2003), Multipoint observations of a Pi2 pulsation on morningside: The 20 September 1995 event, *J. Geophys. Res.*, 108(A5), 1219, doi:10.1029/2002JA009747.

Pashin, A. B., K. H. Glassmeier, W. Baumjohann, O. M. Raspopov, A. G. Yahnin, H. J. Opgenoorth, and R. J. Pellinen (1982), Pi2 magnetic pulsations, auroral break-ups and the substorm current wedge: A case study, *J. Geophys.*, 51, 223–233.

Rostoker, G. (2000), Ground magnetic signatures of ULF and substorm activity during an interval of abnormally weak solar wind on May 11, 1999, *Geophys. Res. Lett.*, 27, 3789–3792.

Russell, C. T. (2000), How northward turnings of the IMF can lead to substorm expansion onsets, *Geophys. Res. Lett.*, 27, 3257–3259.

Russell, C. T., and R. L. McPherron (1973), The magnetotail and substorms, *Space Sci. Rev.*, *15*, 205–266.

Russell, C. T., P. J. Chi, D. J. Dearborn, Y. S. Ge, B. Kuo-Tiong, J. D. Means, D. R. Pierce, K. M. Rowe, and R. C. Snare (2008), THEMIS ground-based magnetometers, *Space Sci. Rev.*, *141*, doi:10.1007/s11214-008-9337-0.

Saito, T. (1969), Geomagnetic pulsations, *Space Sci. Rev.*, *10*, 319–412.

Sakurai, T., and R. L. McPherron (1983), Satellite observations of Pi2 activity at synchronous orbit, *J. Geophys. Res.*, *88*, 7015–7024.

Samson, J. C., and B. G. Harrold (1983), Maps of the polarization of high-latitude Pi2's, *J. Geophys. Res.*, *88*, 5736–5744.

Shiokawa, K., et al. (1998), High-speed ion flow, substorm current wedge, and multiple Pi2 pulsations, *J. Geophys. Res.*, *103*, 4491–4507.

Sutcliffe, P. R. (1998), Observations of Pi2 pulsations in a near ground state, *Geophys. Res. Lett.*, *25*, 4067–4070.

Sutcliffe, P. R., and L. R. Lyons (2002), Association between quiet time Pi2 pulsations, poleward boundary intensifications, and plasma sheet particle fluxes, *Geophys. Res. Lett.*, *29*(9), 1293, doi:10.1029/2001GL014430.

Tsyganenko, N. A. (1989), A magnetospheric magnetic field model with the warped tail current sheet, *Planet. Space Sci.*, *37*, 5–20.

Untiedt, J., and W. Baumjohann (1993), Studies of polar current systems using the IMS scandinavian magnetometer array, *Space Sci. Rev.*, *63*, 245–390.

Yumoto, K. and the CPMN Group (2001), Characteristics of Pi2 magnetic pulsations observed at the CPMN stations: A review of the STEP results, *Earth Planets Space*, *53*, 981–992.

————————————

V. Angelopoulos and C. T. Russell, Institute of Geophysics and Planetary Physics, University of California, Los Angeles, CA 90095, USA.

U. Auster and K. H. Glassmeier, Institute for Geophysics and Extraterrestrial Physics, Technical University of Braunschweig, D-38106 Braunschweig, Germany.

W. Baumjohann, Space Research Institute, Austrian Academy of Sciences, A-8042 Graz, Austria.

C.-C. Cheng, Faculty of Physics, National Formosa University, Hu-Wei 63201, Taiwan. (cccheng@nfu.edu.tw)

I. Mann, Department of Physics, University of Alberta, Edmonton, AB T6G 2J1, Canada.